

Discontinuous finite volume element discretization for coupled flow–transport problems arising in models of sedimentation



Raimund Bürger^{a,*}, Sarvesh Kumar^b, Ricardo Ruiz-Baier^c

^a C²MA and Departamento de Ingeniería Matemática, Universidad de Concepción, Casilla 160-C, Concepción, Chile

^b Department of Mathematics, Indian Institute of Space Science and Technology, Thiruvananthapuram 695 547, Kerala, India

^c Institute of Earth Sciences, Géopolis UNIL-Mouline, University of Lausanne, CH-1015 Lausanne, Switzerland

ARTICLE INFO

Article history:

Received 18 February 2015

Received in revised form 9 July 2015

Accepted 10 July 2015

Available online 14 July 2015

MSC:

65M60
65M12
65M15
35Q35
76D07

Keywords:

Discontinuous finite volume element methods
Semi-discrete scheme
Convergence to the weak solution
Error estimates
Nonlinear coupled flow and transport
Sedimentation–consolidation processes
Gravity flows

ABSTRACT

The sedimentation–consolidation and flow processes of a mixture of small particles dispersed in a viscous fluid at low Reynolds numbers can be described by a nonlinear transport equation for the solids concentration coupled with the Stokes problem written in terms of the mixture flow velocity and the pressure field. Here both the viscosity and the forcing term depend on the local solids concentration. A semi-discrete discontinuous finite volume element (DFVE) scheme is proposed for this model. The numerical method is constructed on a baseline finite element family of linear discontinuous elements for the approximation of velocity components and concentration field, whereas the pressure is approximated by piecewise constant elements. The unique solvability of both the nonlinear continuous problem and the semi-discrete DFVE scheme is discussed, and optimal convergence estimates in several spatial norms are derived. Properties of the model and the predicted space accuracy of the proposed formulation are illustrated by detailed numerical examples, including flows under gravity with changing direction, a secondary settling tank in an axisymmetric setting, and batch sedimentation in a tilted cylindrical vessel.

© 2015 Elsevier Inc. All rights reserved.

1. Introduction

1.1. Scope

The numerical approximation of macroscopic descriptions of sedimentation processes at low Reynolds numbers is needed in a variety of natural phenomena and industrial processes including wastewater treatment [10,18], mineral processing [50], and gravity currents [48]. The governing partial differential equations typically consist of a nonlinear advection–reaction–diffusion equation for the scalar solids concentration coupled with the Stokes or Navier–Stokes equations with concentration-dependent viscosity. The following model can be regarded as a prototype problem of this kind. Consider an

* Corresponding author.

E-mail addresses: rburger@ing-mat.udec.cl (R. Bürger), sarvesh@iist.ac.in (S. Kumar), ricardo.ruizbaier@unil.ch (R. Ruiz-Baier).

incompressible mixture occupying the domain $\Omega \subset \mathbb{R}^d$, $d = 2$ or $d = 3$. Then the motion of the mixture and the evolution of the solids concentration can be described by the initial-boundary value problem

$$\partial_t \phi - \operatorname{div}(\kappa(\phi) \nabla \phi) + \mathbf{u} \cdot \nabla \phi = \nabla \cdot \mathbf{f}(\phi) \quad \text{in } \Omega \times (0, T), \quad (1.1a)$$

$$-\operatorname{div}(\mu(\phi) \boldsymbol{\varepsilon}(\mathbf{u}) - p \mathbf{I}) - \phi \mathbf{g} = \mathbf{0} \quad \text{in } \Omega \times (0, T), \quad (1.1b)$$

$$\operatorname{div} \mathbf{u} = 0 \quad \text{in } \Omega \times (0, T), \quad (1.1c)$$

$$\mathbf{u} = \mathbf{0} \quad \text{on } \Gamma \times (0, T), \quad (1.1d)$$

$$\phi = 0 \quad \text{on } \Gamma \times (0, T), \quad (1.1e)$$

$$\phi(0) = \phi_0 \quad \text{on } \Omega \times \{0\}. \quad (1.1f)$$

The primal unknowns are the volume averaged flow velocity of the mixture \mathbf{u} , the solids concentration ϕ , and the pressure field p . In addition, $\mu(\phi) \boldsymbol{\varepsilon}(\mathbf{u}) - p \mathbf{I}$ is the Cauchy stress tensor, $\boldsymbol{\varepsilon}(\mathbf{u}) = \frac{1}{2}(\nabla \mathbf{u} + \nabla \mathbf{u}^T)$ is the infinitesimal rate of strain, $\mu = \mu(\phi)$ is the concentration-dependent viscosity, and \mathbf{g} is the gravity acceleration. The material specific diffusion function $\kappa = \kappa(\phi)$ and the flux density vector $\mathbf{f} = \mathbf{f}(\phi)$ are motivated by a sedimentation-consolidation model [12] that has been studied extensively in the one-dimensional case. (Precise assumptions on the model ingredients are stated later.) Clearly, the main challenge for the numerical solution of (1.1) is to handle the coupling between the transport equation (1.1a) for ϕ with the flow model (1.1b), (1.1c) that defines \mathbf{u} and p . Desirable properties of a numerical scheme for the approximate solution of this coupled transport-flow problem include mass conservativity, robustness under various ranges of model parameters and geometry configurations, and amenability to L^2 error analysis. For the solution of (1.1) one must resort to a scheme that combines some of the aforementioned properties. It is the purpose of this paper to advance one such combined or hybrid method, namely the so-called discontinuous finite volume element (DFVE) method, for the discretization of (1.1).

This method was originally introduced for elliptic equations in [53] (see also [5,52]), and later extended to Stokes equations in [30,54]. It can be seen as a combination of discontinuous Galerkin (DG) approximations and finite volume element (FVE) methods, typically regarded as Petrov–Galerkin formulations involving different trial and test spaces (see a review in [17]). Advantages of DFVE formulations include local mass conservativity, flexibility for choosing accurate numerical fluxes, smaller dual control volumes (here called diamonds), and suitability for error analysis in the L^2 -norm. In the formulation advanced herein the transport equation (1.1a) is tested against scalar piecewise constant functions spanned by a basis associated to a diamond dual grid, the momentum equation (1.1b) is tested against vectorial piecewise constants also defined on the diamond mesh, and the mass conservation equation (1.1c) is tested against piecewise constants defined on the primal mesh. Integration by parts on each diamond of the dual mesh yields a finite volume scheme (written in terms of fluxes across dual boundaries). Then, special properties of the lumping operator connecting discrete functions defined on primal and dual meshes allow us to rewrite the formulation completely in terms of volume integrals on the primal elements, except for the mass term accompanying the time derivative of ϕ and the right-hand sides of both (1.1a) and (1.1b). In particular, this implies that the quantities defined on the dual mesh will be accessed only through mass and right-hand side assembly, which are typically performed just once during the entire solution algorithm.

The analysis of equivalent continuous coupled formulations can be found in [36], where the Faedo–Galerkin method is employed to establish the weak solvability of the system. Here, the well-posedness analysis of the discrete problem is based on a cut-off of the velocity combined with the properties of the transfer operator between primal and dual meshes, and Picard's Theorem. Next, classical tools consisting of energy-based methods, duality arguments, and elliptic projections are used to obtain error estimates in the natural norms for all fields.

1.2. Related work

Starting with the seminal work of Cai [13], an abundant body of recent literature is devoted to the analysis of FVE-based methods for the discretization of Stokes equations. Among these we point out that continuous approximations include, for instance, pressure-projection and multiscale stabilized methods [34,40,49], whereas nonconforming and discontinuous schemes include those analyzed e.g. in [16,17,30,54]. Some references address the analysis of continuous FVE methods for nonlinear elliptic [15,33] and parabolic problems [14]. DG methods have also been introduced for such problems; for instance, we refer to [25,39] and the references therein for an extensive survey on DG discretizations of nonlinear elliptic and parabolic problems. Nevertheless, and on the other hand, there are hardly any results available dealing with their DFVE counterparts.

Continuous FVE approximations (or similar concepts) have recently been introduced for coupled flow–transport problems. These include, for instance, Crank–Nicolson projection-stabilized methods applied to thermal convection [37], hybrid methods for general conservation laws [22], and edge-based stabilized methods simulating sedimentation–consolidation processes in Stokes and Navier–Stokes regimes [11,44]. However, fully discontinuous FVE methods have only been proposed and studied in the context of porous media flow, where the transport problem is usually less involved and the flow equations are governed by Darcy-like descriptions [27,28]. Even if the conservation property of FVE methods turns them more suitable for discretizing computational fluid dynamics problems, to our knowledge, not even the DFVE approximation of the

nonlinear transport problem alone has been addressed in the literature. We focus our analysis on semi-discrete approximations (the numerical experiments will be based on a simple backward Euler time advancing scheme), but we stress that the main results could be readily extended to the fully discrete case.

1.3. Outline

We have arranged the remainder of this paper in the following manner. Section 2 contains some basic notation and we state the assumptions on the governing equations, present the concept of weak solution and comment on the solvability of the continuous problem. The DFVE scheme is introduced in Section 3, and we derive optimal error estimates in Section 4. Section 5 contains several numerical results illustrating the behavior of the model, while showing the accuracy and robustness of the formulation.

2. Preliminaries and problem statement

2.1. Notation

By $\Omega \subset \mathbb{R}^d$, $d = 2, 3$ we denote a given open bounded domain with polyhedral boundary Γ , and denote by \mathbf{v} the outward unit normal vector on Γ . Usual notation will be adopted for Lebesgue spaces $L^p(\Omega)$ and Sobolev spaces $H^s(\Omega)$ with norm $\|\cdot\|_{s,\Omega}$ and adopt the convention $H^0(\Omega) := L^2(\Omega)$. By \mathbf{M} we will denote the vectorial counterpart of the generic scalar functional space M . For a time $T > 0$, standard Bochner spaces are denoted by $L^p(0, T; H^m(\Omega))$. As usual, \mathbf{I} stands for the $d \times d$ identity tensor, and for any $\boldsymbol{\tau} = (\tau_{ij})_{i,j=1,\dots,d}$ and any vector field $\mathbf{v} = (v_i)_{i=1,\dots,d}$ we denote

$$\begin{aligned}\boldsymbol{\tau}^\top &= (\tau_{ji}), \quad \text{tr}(\boldsymbol{\tau}) = \sum_{i=1}^d \tau_{ii}, \quad \boldsymbol{\tau} : \boldsymbol{\zeta} = \sum_{i,j=1}^d \tau_{ij} \zeta_{ij}, \quad \operatorname{div} \mathbf{v} = \sum_{i=1}^d \partial_i v_i, \\ \operatorname{div} \boldsymbol{\tau} &= \begin{pmatrix} \partial_1 \tau_{11} + \cdots + \partial_d \tau_{1d} \\ \vdots \\ \partial_1 \tau_{d1} + \cdots + \partial_d \tau_{dd} \end{pmatrix}, \quad \nabla \mathbf{v} = \begin{bmatrix} \partial_1 v_1 & \cdots & \partial_d v_1 \\ \vdots & \ddots & \vdots \\ \partial_1 v_d & \cdots & \partial_d v_d \end{bmatrix}.\end{aligned}$$

By $\mathbb{P}_k(L)$ we denote the space of polynomial functions of total degree $s \leq k$ defined on the generic domain L . In what follows, constants independent of the meshsize will be generically denoted by C .

2.2. Assumptions on the governing equations

We assume that the nonlinear viscosity function μ appearing in (1.1b) satisfies

$$\mu, \mu' \in \operatorname{Lip}(\mathbb{R}_+); \quad \exists \gamma_0, \mu_{\min}, \mu_{\max} > 0 : \forall s \in \mathbb{R}_+ : \mu_{\min} < \mu(s) < \mu_{\max}, |\mu'(s)| \leq \gamma_0. \quad (2.1)$$

Moreover, the flux $\mathbf{f} = \mathbf{f}(\phi)$ is assumed to be Lipschitz continuous, and the diffusion coefficient $\kappa = \kappa(\phi)$ is a nonlinear function satisfying

$$\kappa, \kappa' \in \operatorname{Lip}(\mathbb{R}_+); \quad \exists \gamma_1, \gamma_2, \gamma_3 > 0 : \forall x \in \mathbb{R} : \gamma_1 \leq \kappa(x) \leq \gamma_2, |\kappa'(x)| \leq \gamma_3. \quad (2.2)$$

In the context of sedimentation-consolidation models, the function \mathbf{f} describes the effect of hindered settling aligned with gravity, and is usually given by $\mathbf{f}(\phi) = f_b(\phi)\mathbf{k}$, where f_b denotes the Kynch batch flux density function [9,32] and \mathbf{k} is the upwards-pointing unit vector. The function f_b is given by

$$f_b(\phi) = \begin{cases} -v_\infty \phi V(\phi) & \text{for } 0 \leq \phi \leq \phi_{\max}, \\ 0 & \text{for } \phi < 0 \text{ or } \phi > \phi_{\max}, \end{cases}$$

where v_∞ is the Stokes velocity, that is, the settling velocity of a single particle in an unbounded fluid, ϕ_{\max} denotes a (nominal) maximum solids concentration, and $V(\phi)$ is the so-called hindered settling factor, which can for example be given by $V(\phi) = (1 - \phi/\phi_{\max})^{n_{\text{RZ}}}$, where n_{RZ} is a material-dependent exponent [41]. The function $\kappa = \kappa(\phi)$ models the combined effects of hydrodynamic self-diffusion (see [23,24] and references cited in these works) and sediment compressibility [12]. This function is given by

$$\kappa(\phi) = D_0 - \frac{f_b(\phi)\sigma'_e(\phi)}{(\rho_s - \rho_f)g\phi},$$

where $D_0 > 0$ is the constant of hydrodynamic self-diffusion [45], ρ_s and ρ_f are the (constant) solid and fluid mass densities, respectively, and $\sigma'_e(\phi) = d\sigma_e/d\phi$ is the derivative of the so-called effective solid stress function $\sigma_e = \sigma_e(\phi)$, which characterizes sediment compressibility in the case that particles are flocculated. This function is an optional ingredient of the model, and we assume that $\sigma_e \in C^2(\mathbb{R})$ with $\sigma'_e \geq 0$. Furthermore, the forcing term $\phi\mathbf{g}$, where $\mathbf{g} = g\mathbf{k}$ and g is the acceleration of gravity, models that the mixture flow is driven by local fluctuations of ϕ , and therefore of the density of

the density of the mixture, besides possible inflow and outflow conditions. Finally, as in [11,44], we mention that a suitable choice of $\mu(\phi)$ is

$$\mu(\phi) = (1 - \phi/\tilde{\phi}_{\max})^{-\beta}, \quad (2.3)$$

where the parameter $\tilde{\phi}_{\max}$ is a second (nominal) maximum concentration. If we set $\tilde{\phi}_{\max} > \phi_{\max}$, then (2.1) is indeed satisfied.

2.3. Weak formulation

Multiplication by adequate test functions and integration by parts over Ω and using $\operatorname{div} \mathbf{u} = 0$ yields the following weak formulation to (1.1): For $0 < t < T$, find $(\mathbf{u}(t), p(t), \phi(t)) \in \mathbf{H}_0^1(\Omega) \times L_0^2(\Omega) \times H_0^1(\Omega)$ such that

$$\begin{aligned} \langle \partial_t \phi, \varphi \rangle + A(\phi, \varphi; \phi) + C(\phi, \varphi; \mathbf{u}) - \langle \nabla \cdot \mathbf{f}(\phi), \varphi \rangle &= 0 \quad \forall \varphi \in H_0^1(\Omega), \\ \hat{A}(\mathbf{u}, \mathbf{v}; \phi) - b(\mathbf{v}, p) - d(\phi, \mathbf{v}) &= 0 \quad \forall \mathbf{v} \in \mathbf{H}_0^1(\Omega), \\ b(\mathbf{u}, q) &= 0 \quad \forall q \in L^2(\Omega), \end{aligned} \quad (2.4)$$

and $\phi(0) = \phi_0$ a.e. in Ω , where $\mathbf{H}_0^1(\Omega) := \{\mathbf{v} \in \mathbf{H}^1(\Omega) : \mathbf{v}|_\Gamma = 0\}$, $L_0^2(\Omega) := \{q \in L^2(\Omega) : \int_\Omega q \, dx = 0\}$, $H_\Gamma^1(\Omega) := \{s \in H^1(\Omega) : s|_\Gamma = 0\}$ and the involved trilinear (uppercase letters) and bilinear (lowercase) forms are defined as

$$\begin{aligned} \hat{A}(\mathbf{u}, \mathbf{v}; \phi) &:= \int_{\Omega} \mu(\phi) \boldsymbol{\epsilon}(\mathbf{u}) : \boldsymbol{\epsilon}(\mathbf{v}) \, dx, \quad A(\phi, \varphi; \psi) := \int_{\Omega} (\kappa(\psi) \nabla \phi) \cdot \nabla \varphi \, dx, \\ b(\mathbf{v}, q) &:= \int_{\Omega} q \operatorname{div} \mathbf{v} \, dx, \quad C(\phi, \varphi; \mathbf{v}) = - \int_{\Omega} (\mathbf{v} \cdot \nabla \varphi) \phi \, dx, \quad d(\phi, \mathbf{v}) := \int_{\Omega} \phi \mathbf{g} \cdot \mathbf{v} \, dx, \end{aligned}$$

for all $\phi, \varphi, \psi \in H_0^1(\Omega)$, $\mathbf{u}, \mathbf{v} \in \mathbf{H}_0^1(\Omega)$, and $q \in L^2(\Omega)$. These trilinear and bilinear forms satisfy the following stability properties:

Lemma 2.1. For any $\mathbf{u}, \mathbf{v}, \mathbf{w} \in \mathbf{H}^1(\Omega)$, $\phi, \varphi \in H^1(\Omega)$ and $q \in L^2(\Omega)$ there exist constants $C, \beta > 0$ such that

$$\begin{aligned} |A(\phi, \varphi; \cdot)| &\leq C \|\phi\|_{1,\Omega} \|\varphi\|_{1,\Omega}, & |A(\phi, \phi; \cdot)| &\geq C \|\phi\|_{1,\Omega}^2, \\ |\hat{A}(\mathbf{u}, \mathbf{v}; \cdot)| &\leq C \|\mathbf{u}\|_{1,\Omega} \|\mathbf{v}\|_{1,\Omega}, & |\hat{A}(\mathbf{u}, \mathbf{u}; \cdot)| &\geq C \|\mathbf{u}\|_{1,\Omega}^2, \\ |b(\mathbf{v}, q)| &\leq C \|\mathbf{v}\|_{1,\Omega} \|q\|_{0,\Omega}, & \sup_{\mathbf{v} \in \mathbf{H}_0^1(\Omega) \setminus \{\mathbf{0}\}} \frac{b(\mathbf{v}, q)}{\|\mathbf{v}\|_{1,\Omega}} &\geq \beta \|q\|_{0,\Omega}. \\ |d(\phi, \mathbf{v})| &\leq C \|\phi\|_{1,\Omega} \|\mathbf{v}\|_{1,\Omega}, \end{aligned}$$

The weak solvability of the nonlinear problem (1.1) was established in [36].

Lemma 2.2. Let $0 \leq \phi_0 \leq \phi_{\max}$, $\phi_0 \in L^\infty(\Omega)$, and assume that $\int_0^\phi \kappa(s) \, ds \in L^2(0, T; H^1(\Omega))$ for $\phi \in H^1(\Omega)$. Then there exists a unique solution to (2.4) satisfying $\phi \in L^2(0, T; H^1(\Omega)) \cap C([0, T]; L^2(\Omega))$ and $\partial_t \phi \in L^2(0, T; H^1(\Omega))$.

3. Finite volume element discretization

3.1. A baseline FE discretization

Let \mathcal{T}_h be a regular, quasi-uniform triangulation of Ω formed by closed triangular (tetrahedral if $d = 3$) elements K with boundary ∂K and diameter h_K and by vertices s_j , $j = 1, \dots, N_h$ with meshsize $h := \max_{K \in \mathcal{T}_h} (h_K)$. Each face σ between two neighboring elements K and L has diameter h_σ . The set of all faces in \mathcal{T}_h is denoted by \mathcal{E}_h , and \mathcal{E}_h^Γ is its restriction to boundary faces. Let h_σ denote the length of the edge e (area of the face in case of 3D). Then it is clear that

$$h_\sigma \leq h_K^{d-1} \leq h^{d-1}. \quad (3.1)$$

We define the following finite element spaces associated to the mesh \mathcal{T}_h :

$$\begin{aligned} \mathcal{V}_h &:= \{\mathbf{v} \in \mathbf{L}^2(\Omega) : \mathbf{v}|_K \in \mathbb{P}_1(K)^d, \forall K \in \mathcal{T}_h\}, & \mathcal{Q}_h &:= \{q \in L_0^2(\Omega) : q|_K \in \mathbb{P}_0(K), \forall K \in \mathcal{T}_h\}, \\ \mathcal{S}_h &:= \{\varphi \in L^2(\Omega) : \varphi|_K \in \mathbb{P}_1(K), \forall K \in \mathcal{T}_h\}, \end{aligned}$$

for the approximation of the velocity \mathbf{v} , the pressure p and the concentration ϕ , respectively.

Let $\mathbf{n}_{K,\sigma}$ denote the outward vector of $K \in \mathcal{T}_h$ normal to $\sigma \subset \partial K$. For a scalar function $q \in L^2(\Omega)$ we let $\llbracket q \rrbracket_\sigma := q|_{\partial K} \mathbf{n}_{K,\sigma} + q|_{\partial L} \mathbf{n}_{L,\sigma}$ denote a vector jump across the face $\sigma = \bar{K} \cap \bar{L}$, and $\{q\}_\sigma$ denote its average value on σ . If $\sigma \in \mathcal{E}_h^\Gamma$, then we simply consider $\llbracket q \rrbracket_\sigma = \{q\}_\sigma = q|_\sigma$.

3.2. Statement of the FVE method and technical results

We define a FVE discretization of the governing equations on Ω following [11,27,54]. To this end, we introduce a so-called diamond mesh \mathcal{T}_h^\sharp consisting of diamonds D_σ generated by barycentric subdivision, which means that each diamond $D_\sigma \in \mathcal{T}_h^\sharp$ is associated to the face $\sigma \in \mathcal{E}_h$ and constructed by joining the barycenters b_K and b_L of the elements K and L sharing the interior face σ , with the vertices of σ .

The transfer between meshes represents a projection of the FE spaces for the approximation of velocity and concentration defined above, on the following finite-dimensional spaces:

$$\mathcal{V}_h^\sharp := \{\mathbf{v} \in \mathbf{L}^2(\Omega) : \mathbf{v}|_{D_\sigma} \in \mathbb{P}_0(D_\sigma)^d \forall D_\sigma \in \mathcal{T}_h^\sharp\}.$$

$$\mathcal{S}_h^\sharp := \{\varphi \in L^2(\Omega) : \varphi|_{D_\sigma} \in \mathbb{P}_0(D_\sigma) \forall D_\sigma \in \mathcal{T}_h^\sharp\}.$$

Let $\mathcal{V}(h) := \mathcal{V}_h + (\mathbf{H}^2(\Omega) \cap \mathbf{H}_0^1(\Omega))$ and $\mathcal{S}(h) := \mathcal{S}_h + (H^2(\Omega) \cap H_0^1(\Omega))$. In order to connect $\mathcal{V}(h)$ to \mathcal{V}_h^\sharp and $\mathcal{S}(h)$ to \mathcal{S}_h^\sharp , respectively, we define the projection maps $\mathcal{P}^\sharp : \mathcal{V}(h) \rightarrow \mathcal{V}_h^\sharp$ and $\mathcal{R}^\sharp : \mathcal{S}(h) \rightarrow \mathcal{S}_h^\sharp$ as follows:

$$\mathcal{P}^\sharp \mathbf{v}|_{D_\sigma} = \frac{1}{h_\sigma} \int_{\sigma} \mathbf{v}|_{D_\sigma} \, ds, \quad \mathcal{R}^\sharp \psi|_{D_\sigma} = \frac{1}{h_\sigma} \int_{\sigma} \psi|_{D_\sigma} \, ds, \quad D_\sigma \in \mathcal{T}_h^\sharp.$$

The construction of the dual mesh \mathcal{T}_h^\sharp and an application of quadrature formulas enables us to state the following technical lemma, which formulates the properties of these operators (see proofs in e.g. [27,29]):

Lemma 3.1. Let $\mathbf{v}_h \in \mathcal{V}_h$, $\varphi_h, \psi_h \in \mathcal{S}_h$, with ψ_h also in $H^2(K)$, and let $K \in \mathcal{T}_h$ and $\sigma \subset \partial K$. Then the following properties are satisfied:

$$\int_{\sigma} (\varphi_h - \mathcal{R}^\sharp \varphi_h) \, ds = 0, \quad \int_{\sigma} (\mathbf{v}_h - \mathcal{P}^\sharp \mathbf{v}_h) \, ds = 0, \quad (3.2)$$

$$\int_K (\varphi_h - \mathcal{R}^\sharp \varphi_h) \, dx = 0, \quad \int_K (\mathbf{v}_h - \mathcal{P}^\sharp \mathbf{v}_h) \, dx = 0, \quad (3.3)$$

$$\|\mathbf{v}_h - \mathcal{P}^\sharp \mathbf{v}_h\|_{0,K} \leq Ch_K |\mathbf{v}_h|_{1,K}, \quad \|\varphi_h - \mathcal{R}^\sharp \varphi_h\|_{0,K} \leq Ch_K |\varphi_h|_{1,K}, \quad (3.4)$$

$$[\![\psi_h]\!]_{\sigma} = \mathbf{0} \Rightarrow [\![\mathcal{R}^\sharp \psi_h]\!]_{\sigma} = \mathbf{0}, \quad [\![\mathbf{v}_h]\!]_{\sigma} = \mathbf{0} \Rightarrow [\![\mathcal{P}^\sharp \mathbf{v}_h]\!]_{\sigma} = \mathbf{0}, \quad (3.5)$$

$$\int_{\sigma} |(\varphi_h - \mathcal{R}^\sharp \varphi_h)| \, ds \leq Ch \|\psi\|_{p,K} \|\varphi_h\|_{p'} \quad \forall \psi \in H_p^1(K), \quad \varphi_h \in \mathcal{S}_h, \quad \frac{1}{p} + \frac{1}{p'} = 1, \quad (3.6)$$

$$\|\mathcal{P}^\sharp \mathbf{v}_h\|_{0,\Omega} = \|\mathbf{v}_h\|_{0,\Omega}, \quad \|\mathcal{R}^\sharp \varphi_h\|_{0,\Omega} = \|\varphi_h\|_{0,\Omega}. \quad (3.7)$$

Let $\varphi_h \in \mathcal{S}_h$, $\mathbf{v}_h \in \mathcal{V}_h$, $q_h \in \mathcal{Q}_h$ be suitable test functions. We proceed to multiply the concentration equation (1.1a) and the momentum equation (1.1b) by $\mathcal{R}^\sharp \varphi_h \in \mathcal{S}_h^\sharp$ and $\mathcal{P}^\sharp \mathbf{v}_h \in \mathcal{V}_h^\sharp$, respectively, and integrating by parts the respective results over each diamond $D_\sigma \in \mathcal{T}_h^\sharp$; and to multiply the mass conservation equation by q_h and integrating by parts the result over $K \in \mathcal{T}_h$. Adding the resulting local conservation equations we end up with a variational formulation written in the form:

Find (ϕ, \mathbf{u}, p) such that

$$\begin{aligned} & \langle \partial_t \phi, \mathcal{R}^\sharp \varphi_h \rangle - \sum_{D_\sigma \in \mathcal{T}_h^\sharp} \int_{\partial D_\sigma} [\kappa(\phi) \nabla \phi - \phi \mathbf{u}] \cdot \mathbf{n} \mathcal{R}^\sharp \varphi_h \, ds = \sum_{D_\sigma \in \mathcal{T}_h^\sharp} \int_{\partial D_\sigma} \mathbf{f}(\phi) \cdot \mathbf{n} \mathcal{R}^\sharp \varphi_h \, ds \quad \forall \varphi_h \in \mathcal{S}_h, \\ & - \sum_{D_\sigma \in \mathcal{T}_h^\sharp} \int_{\partial D_\sigma} \mu(\phi) \boldsymbol{\epsilon}(\mathbf{u}) \mathbf{n} \cdot \mathcal{P}^\sharp \mathbf{v}_h \, ds + \sum_{D_\sigma \in \mathcal{T}_h^\sharp} \int_{\partial D_\sigma} p \mathbf{n} \cdot \mathcal{P}^\sharp \mathbf{v}_h \, ds = d(\phi, \mathcal{P}^\sharp \mathbf{v}_h) \quad \forall \mathbf{v}_h \in \mathcal{V}_h, \\ & b(\mathbf{u}, q_h) = 0 \quad \forall q_h \in \mathcal{Q}_h. \end{aligned} \quad (3.8)$$

Now let $D_{\sigma_j} \in \mathcal{T}_h^\sharp$, with $j = 1, \dots, d+1$, be the $d+1$ sub-elements (triangles if $d=2$, or tetrahedra if $d=3$) contained in element K of the primal mesh \mathcal{T}_h , as sketched in Fig. 1. It follows that

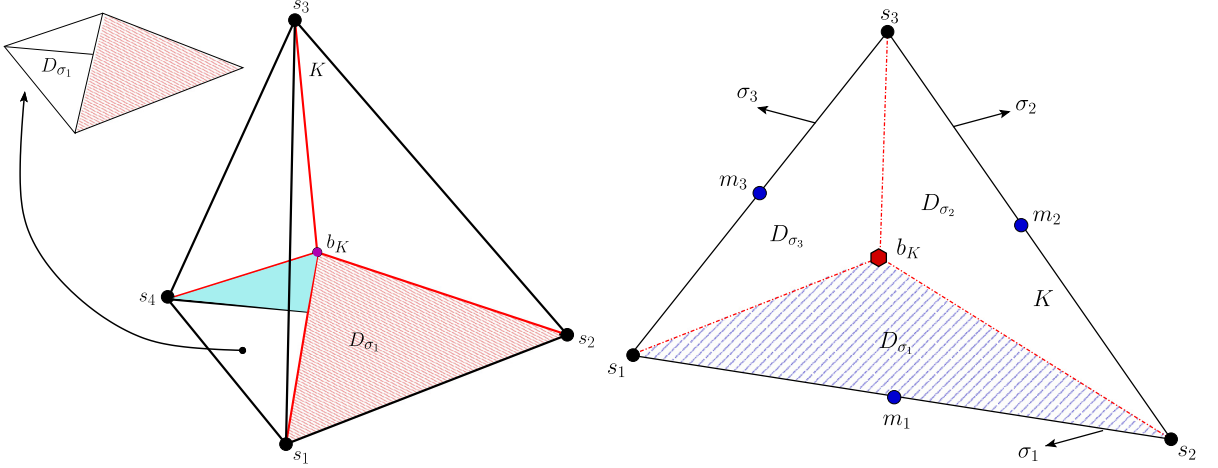


Fig. 1. Left: Tetrahedral element $K \in \mathcal{T}_h$ (solid lines) with barycenter b_K , subdivided into four diamonds D_{σ_j} (dashed lines), where D_{σ_1} is highlighted for sake of visualization. Right: Two-dimensional counterpart, including also the three midpoints m_j of each edge σ_j .

$$\begin{aligned} \sum_{D_\sigma \in \mathcal{T}_h^\sharp} \int_{\partial D_\sigma} [\kappa(\phi) \nabla \phi - \phi \mathbf{u}] \cdot \mathbf{n} \mathcal{R}^\sharp \varphi_h \, ds &= \sum_{K \in \mathcal{T}_h} \sum_{j=1}^{d+1} \int_{\partial D_{\sigma_j}} [\kappa(\phi) \nabla \phi - \phi \mathbf{u}] \cdot \mathbf{n} \mathcal{R}^\sharp \varphi_h \, ds \\ &= \sum_{K \in \mathcal{T}_h} \sum_{j=1}^{d+1} \int_{s_{j+1} b_K s_j} (\kappa(\phi) \nabla \phi - \phi \mathbf{u}) \cdot \mathbf{n} \mathcal{R}^\sharp \varphi_h \, ds \\ &\quad + \sum_{K \in \mathcal{T}_h} \int_{\partial K} (\kappa(\phi) (\nabla \phi) - \phi \mathbf{u} \cdot \mathbf{n}) \mathcal{R}^\sharp \varphi_h \, ds \end{aligned}$$

where $s_{d+2} = s_1$. Similarly, we can assert that

$$\begin{aligned} \sum_{D_\sigma \in \mathcal{T}_h^\sharp} \int_{\partial D_\sigma} \mu(\phi) \boldsymbol{\epsilon}(\mathbf{u}) \mathbf{n} \cdot \mathcal{P}^\sharp \mathbf{v}_h \, ds &= \sum_{K \in \mathcal{T}_h} \sum_{j=1}^{d+1} \int_{s_{j+1} b_K s_j} \mu(\phi) \boldsymbol{\epsilon}(\mathbf{u}) \mathbf{n} \cdot \mathcal{P}^\sharp \mathbf{v}_h \, ds + \sum_{K \in \mathcal{T}_h} \int_{\partial K} \mu(\phi) \boldsymbol{\epsilon}(\mathbf{u}) \mathbf{n} \cdot \mathcal{P}^\sharp \mathbf{v}_h \, ds, \\ \sum_{D_\sigma \in \mathcal{T}_h^\sharp} \int_{\partial D_\sigma} p \mathbf{n} \cdot \mathcal{P}^\sharp \mathbf{v}_h \, ds &= \sum_{K \in \mathcal{T}_h} \sum_{j=1}^{d+1} \int_{s_{j+1} b_K s_j} p \mathbf{n} \cdot \mathcal{P}^\sharp \mathbf{v}_h \, ds + \sum_{K \in \mathcal{T}_h} \int_{\partial K} p \mathbf{n} \cdot \mathcal{P}^\sharp \mathbf{v}_h \, ds, \\ \sum_{D_\sigma \in \mathcal{T}_h^\sharp} \int_{\partial D_\sigma} \mathbf{f}(\phi) \cdot \mathbf{n} \mathcal{R}^\sharp \varphi_h \, ds &= \sum_{K \in \mathcal{T}_h} \sum_{j=1}^{d+1} \int_{s_{j+1} b_K s_j} \mathbf{f}(\phi) \cdot \mathbf{n} \mathcal{R}^\sharp \varphi_h \, ds + \sum_{K \in \mathcal{T}_h} \int_{\partial K} \mathbf{f}(\phi) \cdot \mathbf{n} \mathcal{R}^\sharp \varphi_h \, ds. \end{aligned}$$

Let us next define the following forms for all $\psi_h, \varphi_h, \chi_h \in \mathcal{S}_h$, $\mathbf{w}_h, \mathbf{v}_h \in \mathcal{V}_h$ and $r_h, q_h \in \mathcal{Q}_h$:

$$\begin{aligned} \mathcal{A}_h^1(\psi_h, \varphi_h; \chi_h, \mathbf{v}_h) &:= - \sum_{K \in \mathcal{T}_h} \sum_{j=1}^{d+1} \int_{s_{j+1} b_K s_j} (\kappa(\chi_h) \nabla \psi_h - \psi_h \mathbf{v}_h) \cdot \mathbf{n} \mathcal{R}^\sharp \varphi_h \, ds, \\ \hat{\mathcal{A}}_h^1(\mathbf{w}_h, \mathbf{v}_h; \psi_h) &:= - \sum_{K \in \mathcal{T}_h} \sum_{j=1}^{d+1} \int_{s_{j+1} b_K s_j} \mu(\psi_h) \boldsymbol{\epsilon}(\mathbf{w}_h) \mathbf{n} \cdot \mathcal{P}^\sharp \mathbf{v}_h \, ds, \\ c_h^1(\mathbf{v}_h, r_h) &:= \sum_{K \in \mathcal{T}_h} \sum_{j=1}^{d+1} \int_{s_{j+1} b_K s_j} r_h \mathbf{n} \cdot \mathcal{P}^\sharp \mathbf{v}_h \, ds, \\ l_h^1(\psi_h; \varphi_h) &:= \sum_{K \in \mathcal{T}_h} \sum_{j=1}^{d+1} \int_{s_{j+1} b_K s_j} \mathbf{f}(\psi_h) \cdot \mathbf{n} \mathcal{R}^\sharp \varphi_h \, ds. \end{aligned}$$

Regularity assumptions on the exact solutions to the continuous problem imply, in particular, that

$$[\kappa(\phi)(\nabla\phi \cdot \mathbf{n})]_\sigma = 0, \quad [\mu(\phi)\boldsymbol{\varepsilon}(\mathbf{u})\mathbf{n}]_\sigma = 0, \quad [\phi(\mathbf{u} \cdot \mathbf{n})]_\sigma = 0, \quad \text{and} \quad [p]_\sigma = 0.$$

Then, using definitions of sums and averages and integration by parts, we can rewrite the integrals initially defined on the elements boundary ∂K , in terms of $[\cdot]_\sigma$ and $\{\cdot\}_\sigma$. This derivation yields the following semi-discrete DFVE formulation associated to the weak formulation (3.8): For all $0 < t < T$, find $(\phi_h(t), \mathbf{u}_h(t), p_h(t)) \in \mathcal{S}_h \times \mathcal{V}_h \times \mathcal{Q}_h$ such that

$$\langle \partial_t \phi_h, \mathcal{R}^\sharp \varphi_h \rangle + \mathcal{A}_h(\phi_h(t), \varphi_h; \phi_h(t), \mathbf{u}_h(t)) = l_h(\phi_h(t); \varphi_h) \quad \forall \varphi_h \in \mathcal{S}_h, \quad (3.9)$$

$$\hat{\mathcal{A}}_h(\mathbf{u}_h(t), \mathbf{v}_h; \phi_h(t)) + c_h(\mathbf{v}_h, p_h(t)) = d(\phi_h(t), \mathcal{P}^\sharp \mathbf{v}_h) \quad \forall \mathbf{v}_h \in \mathcal{V}_h, \quad (3.10)$$

$$b_h(\mathbf{u}_h(t), q_h) = 0 \quad \forall q_h \in \mathcal{Q}_h, \quad (3.11)$$

where we define

$$\begin{aligned} \mathcal{A}_h(\psi_h, \varphi_h; \chi_h, \mathbf{w}_h) &:= \mathcal{A}_h^1(\psi_h, \varphi_h; \chi_h, \mathbf{w}_h) - \sum_{\sigma \in \mathcal{E}_h} \int_{\sigma} \{(\kappa(\chi_h) \nabla \psi_h - \psi_h \mathbf{w}_h) \cdot \mathbf{n}\}_\sigma \cdot [\mathcal{R}^\sharp \varphi_h]_\sigma \, ds \\ &\quad - \sum_{\sigma \in \mathcal{E}_h} \int_{\sigma} \{\kappa(\chi_h) (\nabla \varphi_h \cdot \mathbf{n})\}_\sigma \cdot [\mathcal{R}^\sharp \psi_h]_\sigma \, ds + \sum_{\sigma \in \mathcal{E}_h} \int_{\sigma} \frac{\alpha_c}{h_\sigma^\delta} [\psi_h]_\sigma \cdot [\varphi_h]_\sigma \, ds, \\ \hat{\mathcal{A}}_h(\mathbf{w}_h, \mathbf{v}_h; \psi_h) &:= \hat{\mathcal{A}}_h^1(\mathbf{w}_h, \mathbf{v}_h; \psi_h) - \sum_{\sigma \in \mathcal{E}_h} \int_{\sigma} \{\mu(\psi_h) \boldsymbol{\varepsilon}(\mathbf{w}_h) \mathbf{n}\}_\sigma \cdot [\mathcal{P}^\sharp \mathbf{v}_h]_\sigma \, ds \\ &\quad - \sum_{\sigma \in \mathcal{E}_h} \int_{\sigma} \{\mu(\psi_h) \boldsymbol{\varepsilon}(\mathbf{v}_h) \mathbf{n}\}_\sigma \cdot [\mathcal{P}^\sharp \mathbf{w}_h]_\sigma \, ds + \sum_{\sigma \in \mathcal{E}_h} \int_{\sigma} \frac{\alpha_d}{h_\sigma^\delta} [\mathbf{w}_h]_\sigma \cdot [\mathbf{v}_h]_\sigma \, ds, \\ l_h(\psi_h; \varphi_h) &:= l_h^1(\psi_h; \varphi_h) + \sum_{\sigma \in \mathcal{E}_h} \int_{\sigma} \{\mathbf{f}(\psi_h) \cdot \mathbf{n}\}_\sigma [\varphi_h]_\sigma \, ds, \\ c_h(\mathbf{v}_h, r_h) &:= c_h^1(\mathbf{v}_h, r_h) + \sum_{\sigma \in \mathcal{E}_h} \int_{\sigma} \{r_h\}_\sigma [\mathbf{v}_h]_\sigma \, ds, \\ b_h(\mathbf{w}_h, q_h) &:= b(\mathbf{w}_h, q_h) - \sum_{\sigma \in \mathcal{E}_h} \int_{\sigma} \{q_h\}_\sigma [\mathbf{w}_h]_\sigma \, ds. \end{aligned}$$

Here, α_c and α_d are nonnegative penalty parameters that will be specified later and δ depends on the dimension d . We set $\delta = (d-1)^{-1}$, as usually done in case of DG methods. For our future analysis we also define the following natural mesh-dependent norms for all $\psi_h \in \mathcal{S}(h)$ and $\mathbf{v}_h \in \mathcal{V}(h)$:

$$\begin{aligned} \|\psi_h\|_h^2 &:= \sum_{K \in \mathcal{T}_h} \|\nabla \psi_h\|_{0,K}^2 + \sum_{\sigma \in \mathcal{E}_h} h_\sigma^{-\delta} \|[\psi_h]_\sigma\|_{0,\sigma}^2, \quad \|\psi_h\|^2 := \|\psi_h\|_h^2 + \sum_{K \in \mathcal{T}_h} h_K^2 |\psi_h|_{2,K}^2, \\ \|\mathbf{v}_h\|_h^2 &:= \sum_{K \in \mathcal{T}_h} |\mathbf{v}_h|_{1,K}^2 + \sum_{\sigma \in \mathcal{E}_h} h_\sigma^{-\delta} \|[\mathbf{v}_h]_\sigma\|_{0,\sigma}^2, \quad \|\mathbf{v}_h\|_{1,h}^2 := \|\mathbf{v}_h\|_h^2 + \sum_{K \in \mathcal{T}_h} h_K^2 |\mathbf{v}_h|_{2,K}^2. \end{aligned}$$

The standard inverse inequality implies that there exists $C > 0$ such that

$$\|\varphi_h\| \leq C \|\varphi_h\|_h \quad \forall \varphi_h \in \mathcal{S}_h, \quad \|\mathbf{v}_h\|_{1,h} \leq C \|\mathbf{v}_h\|_h \quad \forall \mathbf{v}_h \in \mathcal{V}_h. \quad (3.12)$$

A simple application of the Gauss divergence theorem provides the following result.

Lemma 3.2. *The following relations hold for all $\psi_h, \varphi_h, \chi_h \in \mathcal{S}_h$, $\mathbf{w}_h, \mathbf{v}_h \in \mathcal{V}_h$, and $q_h \in \mathcal{Q}_h$.*

$$\begin{aligned} -\mathcal{A}(\psi_h, \varphi_h; \chi_h) &= \sum_{K \in \mathcal{T}_h} \sum_{j=1}^{d+1} \int_{s_{j+1} b_K s_j} (\kappa(\chi_h) \nabla \psi_h) \cdot \mathbf{n} \mathcal{R}^\sharp \varphi_h \, ds \\ &\quad + \sum_{K \in \mathcal{T}_h} \int_{\partial K} (\kappa(\chi_h) \nabla \psi_h) \cdot \mathbf{n} (\mathcal{R}^\sharp \varphi_h - \varphi_h) \, ds \\ &\quad + \sum_{K \in \mathcal{T}_h} \int_K \nabla \cdot (\kappa(\chi_h) \nabla \psi_h) (\varphi_h - \mathcal{R}^\sharp \varphi_h) \, dx, \end{aligned} \quad (3.13)$$

$$\begin{aligned} \hat{\mathcal{A}}_h^1(\mathbf{w}_h, \mathbf{v}_h; \psi_h) &= \hat{\mathcal{A}}(\mathbf{w}_h, \mathbf{v}_h; \psi_h) + \sum_{K \in \mathcal{T}_h} \int_{\partial K} \mu(\psi_h) (\mathcal{P}^\sharp \mathbf{v}_h - \mathbf{v}_h) \boldsymbol{\varepsilon}(\mathbf{w}_h) : \mathbf{n} \, ds \\ &\quad + \sum_{K \in \mathcal{T}_h} \int_K \nabla \cdot (\mu(\psi_h) \boldsymbol{\varepsilon}(\mathbf{w}_h)) \cdot (\mathbf{v}_h - \mathcal{P}^\sharp \mathbf{v}_h) \, dx, \end{aligned} \quad (3.14)$$

$$c_h^1(\mathbf{v}_h, q_h) = -b(\mathbf{v}_h, q_h). \quad (3.15)$$

Proof. Relations (3.13) and (3.14) follow as in [53, p. 1067], whereas (3.15) can be established using [54, p. 189]. \square

4. Solvability and convergence analysis

In this section and also in subsequent sections, we assume that $\mathbf{u}(t) \in L^\infty(\Omega)$ and make use of the Lipschitz continuity and boundedness assumptions (given in (2.1) and (2.2)) on viscosity $\mu = \mu(\phi)$, flux function $\mathbf{f} = \mathbf{f}(\phi)$ and diffusion coefficient $\kappa = \kappa(\phi)$. We also use the following well known inverse inequalities $\forall \mathbf{v}_h \in \mathcal{V}_h$:

$$\|\mathbf{v}_h\|_{1,K} \leq Ch_K^{-1}\|\mathbf{v}_h\|_{0,K}, \quad \|\mathbf{v}_h\|_{\infty,K} \leq Ch_K^{-d/2}\|\mathbf{v}_h\|_{0,K}, \quad \|\nabla \mathbf{v}_h\|_{\infty,K} \leq h_K^{-d/2}\|\nabla \mathbf{v}_h\|_{0,K}, \quad (4.1)$$

$$\|\mathbf{v}_h\|_{0,\sigma} \leq Ch_K^{-1/2}\|\mathbf{v}_h\|_{0,K}, \quad \|(\nabla \mathbf{v}_h)\mathbf{n}_{K,\sigma}\|_{0,\sigma} \leq Ch_K^{-1/2}\|\nabla \mathbf{v}_h\|_{0,K}. \quad (4.2)$$

The scalar version of the inequalities stated in (4.1) and (4.2) is given in [19] and Lemma 2.1 of [42], respectively. In addition, we will also frequently use the following well-established trace inequalities (cf. [1, Th. 3.10]):

$$\begin{aligned} \|\mathbf{v}\|_{0,\sigma}^2 &\leq C(h_K^{-1}\|\mathbf{v}\|_{0,K}^2 + h_K|\mathbf{v}|_{1,K}^2) \quad \forall \mathbf{v} \in \mathbf{H}^1(K), \\ \|(\nabla \mathbf{v})\mathbf{n}_{K,\sigma}\|_{0,\sigma}^2 &\leq C(h_K^{-1}|\mathbf{v}|_{1,K}^2 + h_K|\mathbf{v}|_{2,K}^2) \quad \forall \mathbf{v} \in \mathbf{H}^2(K), \end{aligned} \quad (4.3)$$

for $\sigma \subset \partial K$, where $C > 0$ depends also on the minimum angle of $K \in \mathcal{T}_h$.

4.1. Solvability

Let us define the following “cut-off” operator \mathcal{N} for the velocity (see [47]):

$$\mathcal{N}(\mathbf{u})(x) := \min\{|\mathbf{u}(x)|, N\} \frac{\mathbf{u}(x)}{|\mathbf{u}(x)|},$$

where N is a fixed positive number and $|\mathbf{u}(x)| = (\sum_{i=1}^d u_i(x)^2)^{1/2}$. The map \mathcal{N} is uniformly bounded and uniformly Lipschitz continuous (see [47, p. 331]), i.e.,

$$\|\mathcal{N}(\mathbf{u}) - \mathcal{N}(\mathbf{v})\|_{\infty,\Omega} \leq \|\mathbf{u} - \mathbf{v}\|_{\infty,\Omega}. \quad (4.4)$$

For now let us denote $\mathcal{N}(\mathbf{u}_h)(x)$ as \mathbf{u}_h^N . It is still left to precisely define this “cut-off” operator, but for the moment it suffices to note that in the subsequent analysis we will require the computed velocity \mathbf{u}_h to be uniformly bounded, which can be guaranteed by the definition of \mathcal{N} .

For a fixed ϕ_h , an application of (3.13), (3.2), (3.3) helps us to show that the bilinear form $\hat{A}_h(\cdot, \cdot; \phi_h)$ is coercive with respect to $\|\cdot\|_h$, i.e., there exists a positive constant α independent of the mesh size h such that for α_d large enough and h small enough

$$\hat{A}_h(\mathbf{v}_h, \mathbf{v}_h; \phi_h) \geq \alpha \|\mathbf{v}_h\|_h^2. \quad (4.5)$$

For a detailed proof and restrictions on the penalty parameter α_d , we refer to [54, Lemma 3.5]; see also [29]. Moreover, the choice of finite element spaces \mathcal{V}_h and \mathcal{Q}_h yields the inf-sup condition [54]

$$\sup_{\mathbf{v}_h \in \mathcal{V}_h} \frac{b_h(\mathbf{v}_h, q_h)}{\|\mathbf{v}_h\|_h} \geq \beta_1 \|q_h\|_{0,\Omega}, \quad (4.6)$$

where $\beta_1 > 0$ is independent of h . Hence, using (3.15) and the Babuška–Brezzi theory for saddle point problems we can assert that, for a given ϕ_h , there exists a unique solution to the flow equations (3.10), (3.11). In particular, the existence of \mathbf{u}_h implies that of \mathbf{u}_h^N . To prove the existence and uniqueness of ϕ_h (and also in view of the error analysis to be presented later on), it is convenient to recast (3.9) employing the definition of $\mathcal{A}_h(\cdot, \cdot; \cdot, \cdot)$ in the following manner:

Find $\phi_h \in \mathcal{S}_h$ such that

$$\begin{aligned} \langle \partial_t \phi_h, \mathcal{R}^\sharp \varphi_h \rangle + B_h(\phi_h, \varphi_h; \chi_h) &= - \sum_{K \in \mathcal{T}_h} \sum_{j=1}^{d+1} \int_{s_{j+1} b_K s_j} \mathbf{u}_h^N \cdot \mathbf{n} \phi_h \mathcal{R}^\sharp \varphi_h \, ds \\ &\quad - \sum_{\sigma \in \mathcal{E}_h} \int_{\sigma} \{\mathbf{u}_h^N \cdot \mathbf{n} \phi_h\}_{\sigma} \cdot [\mathcal{R}^\sharp \varphi_h]_{\sigma} \, ds + l_h(\phi_h; \varphi_h) \quad \forall \varphi_h \in \mathcal{S}_h, \end{aligned} \quad (4.7)$$

where

$$\begin{aligned} B_h(\psi_h, \varphi_h; \chi_h) := & - \sum_{K \in \mathcal{T}_h} \sum_{j=1}^{d+1} \int_{s_{j+1} b_K s_j} (\kappa(\chi_h) \nabla \psi_h) \cdot \mathbf{n} \mathcal{R}^\sharp \varphi_h \, ds + \sum_{\sigma \in \mathcal{E}_h} \int_{\sigma} \frac{\alpha_c}{h_\sigma^\delta} [\![\psi_h]\!]_\sigma \cdot [\![\varphi_h]\!]_\sigma \, ds \\ & - \sum_{\sigma \in \mathcal{E}_h} \int_{\sigma} \{(\kappa(\chi_h) \nabla \psi_h) \cdot \mathbf{n}\}_\sigma \cdot [\![\mathcal{R}^\sharp \varphi_h]\!]_\sigma \, ds - \sum_{\sigma \in \mathcal{E}_h} \int_{\sigma} \{\kappa(\chi_h) (\nabla \varphi_h \cdot \mathbf{n})\}_\sigma \cdot [\![\mathcal{R}^\sharp \psi_h]\!]_\sigma \, ds. \end{aligned}$$

To obtain an *a priori* bound of ϕ_h which will be used for the well-posedness of the system (3.9)–(3.11), below we show that $B_h(\cdot, \cdot, \cdot)$ is coercive and bounded within the ball $B_M = \{\psi_h \in \mathcal{S}_h : \|\nabla \psi_h\|_\infty \leq M\}$.

Lemma 4.1. *There exist generic positive constants β and C independent of h , but which may depend on the penalty parameter α_c , such that*

$$\begin{aligned} B_h(\chi_h, \chi_h; \chi_h) &\geq \beta \|\chi_h\|_h^2 \quad \forall \chi_h \in B_M, \\ |B_h(\psi_h, \varphi_h; \chi_h)| &\leq C \|\psi_h\|_h \|\varphi_h\|_h \quad \forall \psi_h, \varphi_h \in \mathcal{S}_h \quad \forall \chi_h \in B_M. \end{aligned} \quad (4.8)$$

Proof. Define

$$E(\psi_h, \varphi_h; \chi_h) := - \sum_{K \in \mathcal{T}_h} \sum_{j=1}^{d+1} \int_{s_{j+1} b_K s_j} (\kappa(\chi_h) \nabla \psi_h) \cdot \mathbf{n} \mathcal{R}^\sharp \varphi_h \, ds - A(\psi_h, \varphi_h; \chi_h).$$

Now, using relation (3.13) we deduce that

$$\begin{aligned} E(\psi_h, \varphi_h; \chi_h) &= \sum_{K \in \mathcal{T}_h} \int_{\partial K} (\kappa(\chi_h) \nabla \psi_h) \cdot \mathbf{n} (\mathcal{R}^\sharp \varphi_h - \varphi_h) \, ds \\ &\quad + \sum_{K \in \mathcal{T}_h} \int_K \nabla \cdot (\kappa(\chi_h) \nabla \psi_h) (\varphi_h - \mathcal{R}^\sharp \varphi_h) \, dx =: T_1 + T_2. \end{aligned} \quad (4.9)$$

An application of (3.6), (2.2) and using the fact that ψ_h and χ_h are linear on each triangle yields

$$\begin{aligned} \left| \int_{\partial K} \kappa(\chi_h) \nabla \psi_h \cdot \mathbf{n} (\varphi_h - \mathcal{R}^\sharp \varphi_h) \, ds \right| &\leq Ch \|\nabla(\kappa(\chi_h) \nabla \psi_h)\|_{0,K} \|\nabla \varphi_h\|_{0,K} \\ &\leq C\gamma_3 h \|\nabla \chi_h \cdot \nabla \psi_h\|_{0,K} \|\nabla \varphi_h\|_{0,K}. \end{aligned}$$

Using the Hölder inequality, the fact that $\chi_h \in B_M$, and summation over all triangles, we obtain that

$$|T_1| \leq Ch \|\psi_h\|_h \|\varphi_h\|_h. \quad (4.10)$$

For T_2 , first we note that

$$\int_K \nabla \cdot (\kappa(\chi_h) \nabla \psi_h) (\varphi_h - \mathcal{R}^\sharp \varphi_h) \, dx \leq \|\nabla \cdot (\kappa(\chi_h) \nabla \psi_h)\|_{0,K} \|\varphi_h - \mathcal{R}^\sharp \varphi_h\|_{0,K}.$$

Now, by using (3.3), (2.2) and the fact ψ_h is linear on each K , we obtain

$$|T_2| \leq Ch \|\psi_h\|_h \|\varphi_h\|_h. \quad (4.11)$$

Combining the estimates obtained in (4.10) and (4.11) and inserting them in (4.9), we obtain

$$|E(\psi_h, \varphi_h; \chi_h)| \leq Ch \|\psi_h\|_h \|\varphi_h\|_h \quad \forall \varphi_h, \psi_h \in \mathcal{S}_h, \chi_h \in B_M. \quad (4.12)$$

Now using (4.12) and following the proof lines of Lemmas 2.3 and 2.4 in [29], we complete the rest of the proof. \square

Using the trace inequality (4.3) and properties of \mathcal{R}^\sharp , for $\mathbf{u}(t) \in L^\infty(\Omega)$, the following bound has been derived in [27, p. 1364]:

$$\sum_{K \in \mathcal{T}_h} \sum_{j=1}^{d+1} \int_{s_{j+1} b_K s_j} \mathbf{u} \cdot \mathbf{n} \psi_h \mathcal{R}^\sharp \varphi_h \, ds \leq C \|\varphi_h\|_h (\|\psi_h\|_{0,\Omega} + h \|\psi_h\|_h) \quad \forall \psi_h \in \mathcal{S}(h), \forall \varphi_h \in \mathcal{S}_h. \quad (4.13)$$

Since \mathbf{u}_h^N is also uniformly bounded, (4.13) also holds for \mathbf{u}_h^N . An application of the Cauchy–Schwarz inequality and the trace inequality along with the fact that \mathbf{u}_h^N is uniformly bounded yields

$$\int_{\sigma} \{\mathbf{u}_h^N \cdot \mathbf{n}\psi_h\}_{\sigma} \cdot [\![\mathcal{R}^\sharp \varphi_h]\!]_{\sigma} \, ds \leq Ch_{\sigma}^{\delta/2} \left(h_K^{-1/2} \|\psi_h\|_{0,K} + h_K^{1/2} \|\nabla \psi_h\|_{0,K} \right) \frac{1}{h_{\sigma}^{\delta/2}} \|[\![\mathcal{R}^\sharp \varphi_h]\!]_{\sigma}\|_{0,\sigma}.$$

Now, again a repeated application of the Cauchy–Schwarz inequality together with definitions of \mathcal{R}^\sharp enable us to write

$$\begin{aligned} \frac{1}{h_{\sigma}^{\delta/2}} \|[\![\mathcal{R}^\sharp \varphi_h]\!]_{\sigma}\|_{0,\sigma} &= \frac{1}{h_{\sigma}^{\delta/2}} \left(\int_{\sigma} [\![\mathcal{R}^\sharp \varphi_h]\!]_{\sigma}^2 \, ds \right)^{1/2} = \frac{1}{h_{\sigma}^{(\delta-1)/2}} [\![\mathcal{R}^\sharp \varphi_h]\!]_{\sigma} = \frac{1}{h_{\sigma}^{(\delta+1)/2}} \int_{\sigma} [\![\varphi_h]\!]_{\sigma} \, ds \\ &\leq \frac{1}{h_{\sigma}^{(\delta+1)/2}} \left(\int_{\sigma} [\![\varphi_h]\!]_{\sigma}^2 \, ds \right)^{1/2} \left(\int_{\sigma} \, ds \right)^{1/2} = \left(\frac{1}{h_{\sigma}^{\delta}} \int_{\sigma} [\![\varphi_h]\!]_{\sigma}^2 \, ds \right)^{1/2}. \end{aligned} \quad (4.14)$$

Hence,

$$\int_{\sigma} \{\mathbf{u}_h^N \cdot \mathbf{n}\psi_h\}_{\sigma} \cdot [\![\mathcal{R}^\sharp \varphi_h]\!]_{\sigma} \, ds \leq Ch_{\sigma}^{\delta/2} h_K^{-1/2} (\|\psi_h\|_{0,K} + h_K \|\nabla(\phi - \phi_h)\|_{0,K}) \left(\frac{1}{h_{\sigma}^{\delta}} \int_{\sigma} [\![\varphi_h]\!]_{\sigma}^2 \, ds \right)^{1/2}.$$

Using (3.1), summing over all edges and using the definition of the norm $\|\cdot\|_h$, we have for all $\psi_h, \varphi_h \in \mathcal{S}_h$:

$$\sum_{\sigma \in \mathcal{E}_h} \int_{\sigma} \{\mathbf{u}_h^N \cdot \mathbf{n}\psi_h\}_{\sigma} \cdot [\![\mathcal{R}^\sharp \varphi_h]\!]_{\sigma} \, ds \leq C (\|\psi_h\|_{0,\Omega} + h \|\psi_h\|_h) \|\varphi_h\|_h. \quad (4.15)$$

In a similar way, using the Cauchy–Schwarz inequality and the trace inequality (4.3) and the same arguments used in (4.13) and (4.15), we obtain the following estimate

$$|l_h(\psi_h; \varphi_h)| \leq C (\|\psi_h\|_{0,\Omega} + h \|\psi_h\|_h) \|\varphi_h\|_h \quad \forall \psi_h \in \mathcal{S}(h), \forall \varphi_h \in \mathcal{S}_h. \quad (4.16)$$

Now, existence and uniqueness of ϕ_h can be shown as follows. Substituting \mathbf{u}_h^N in (4.7) gives a system of nonlinear differential equations in ϕ_h . Picard's theorem guarantees the existence and uniqueness of ϕ_h in some small interval $(0, t_h)$. To continue the solution an *a priori* bound for ϕ_h is required, which can be derived easily by employing the inequalities (4.13), (4.15), (4.16) and (4.8); for more details, see [27]. Therefore, existence and uniqueness of ϕ_h is ensured in a ball B_M .

4.2. Error estimates for velocity and pressure

For a given ϕ , we define the projection operators $(\tilde{\mathbf{u}}_h, \tilde{p}_h) : (0, T) \rightarrow \mathcal{V}_h \times \mathcal{Q}_h$ as follows:

$$\hat{A}_h(\tilde{\mathbf{u}}_h, \mathbf{v}_h; \phi) + c_h(\mathbf{v}_h, \tilde{p}_h) = d(\phi, \mathcal{P}^\sharp \mathbf{v}_h) \quad \forall \mathbf{v}_h \in \mathcal{V}_h, \quad (4.17)$$

$$b_h(\tilde{\mathbf{u}}_h, q_h) = 0 \quad \forall q_h \in \mathcal{Q}_h. \quad (4.18)$$

In order to make use of some technical results which were established for $d = 2$ and also for the sake of clarity in the presentation, we present our analysis for $d = 2$ and this analysis can be extended to the case for $d = 3$. In this connection, the following estimates for $(\tilde{\mathbf{u}}_h, \tilde{p}_h) \in \mathcal{V}_h \times \mathcal{Q}_h$ can be derived by imitating the analysis of [17] (see also [54]):

$$\|\mathbf{u} - \tilde{\mathbf{u}}_h\|_{0,\Omega} \leq Ch^2 (\|\mathbf{u}\|_{2,\Omega} + \|p\|_{1,\Omega} + \|\phi g\|_{1,\Omega}), \quad (4.19)$$

$$\|\mathbf{u} - \tilde{\mathbf{u}}_h\|_h + \|p - \tilde{p}_h\|_{0,\Omega} \leq Ch (\|\mathbf{u}\|_{2,\Omega} + \|p\|_{1,\Omega}). \quad (4.20)$$

For our subsequent analysis, we need that $\tilde{\mathbf{u}}_h$ is bounded in the following sense:

$$\|\nabla \cdot \tilde{\mathbf{u}}_h\|_{\infty,K} + \|\nabla \cdot \tilde{\mathbf{u}}_h\|_{\infty,\partial K} \leq C \quad \forall K \in \mathcal{T}_h. \quad (4.21)$$

Here, the constant C is independent of h but may depend on the bounds of $\|\mathbf{u}\|_{2,\Omega}$. For the establishment of (4.21), quasi-uniformity of the mesh, (4.19), inverse inequalities (4.1), (4.2) and continuous interpolant approximations properties are used. For details on a scalar version of this result, see [4, Theorem 4.7].

The following lemma provides the error estimates for velocity and pressure in terms of concentration.

Lemma 4.2. *There exists a constant C independent of h , but which may depend on the bound of $\tilde{\mathbf{u}}_h$, such that*

$$\|\mathbf{u} - \mathbf{u}_h\|_{0,\Omega} \leq C \left[h^2 (\|\mathbf{u}\|_{2,\Omega} + \|p\|_{1,\Omega} + \|\phi g\|_{1,\Omega}) + \|\phi - \phi_h\|_{0,\Omega} + h \|\phi - \phi_h\|_h \right],$$

$$\|\mathbf{u} - \mathbf{u}_h\|_h + \|p - \tilde{p}_h\|_{0,\Omega} \leq C \left[h (\|\mathbf{u}\|_{2,\Omega} + \|p\|_{1,\Omega}) + \|\phi - \phi_h\|_{0,\Omega} + h \|\phi - \phi_h\|_h \right].$$

Proof. Write $\mathbf{u} - \mathbf{u}_h = \mathbf{u} - \tilde{\mathbf{u}}_h + \tilde{\mathbf{u}}_h - \mathbf{u}_h$ and $p - p_h = p - \tilde{p}_h + \tilde{p}_h - p_h$. Since estimates for $\mathbf{u} - \tilde{\mathbf{u}}_h$ and $p - \tilde{p}_h$ are given in (4.19) and (4.20), we proceed to find estimates for $\tilde{\mathbf{u}}_h - \mathbf{u}_h$ and $\tilde{p}_h - p_h$. Subtracting (3.10) from (4.17) and (3.11) from (4.18), respectively, we get for all $\mathbf{v}_h \in \mathcal{V}_h$ and $q_h \in \mathcal{Q}_h$

$$\hat{A}_h(\tilde{\mathbf{u}}_h, \mathbf{v}_h; \phi) - \hat{A}_h(\mathbf{u}_h, \mathbf{v}_h; \phi_h) + c_h(\mathbf{v}_h, \tilde{p}_h) - c_h(\mathbf{v}_h, p_h) = d(\phi, \mathcal{P}^\# \mathbf{v}_h) - d(\phi_h, \mathcal{P}^\# \mathbf{v}_h), \quad (4.22)$$

$$b_h(\tilde{\mathbf{u}}_h - \mathbf{u}_h, q_h) = 0. \quad (4.23)$$

We rewrite (4.22) as follows:

$$\begin{aligned} \hat{A}_h(\tilde{\mathbf{u}}_h - \mathbf{u}_h, \mathbf{v}_h; \phi_h) + c_h(\mathbf{v}_h, \tilde{p}_h - p_h) &= \hat{A}_h(\tilde{\mathbf{u}}_h, \mathbf{v}_h; \phi_h) - \hat{A}_h(\tilde{\mathbf{u}}_h, \mathbf{v}_h; \phi) \\ &\quad + d(\phi, \mathcal{P}^\# \mathbf{v}_h) - d(\phi_h, \mathcal{P}^\# \mathbf{v}_h) \quad \forall \mathbf{v}_h \in \mathcal{V}_h. \end{aligned} \quad (4.24)$$

By using the definition of $\hat{A}_h(\cdot, \cdot; \cdot)$, (3.14) and the fact that $\tilde{\mathbf{u}}_h$ is linear on K , we can write

$$\begin{aligned} &\hat{A}_h(\tilde{\mathbf{u}}_h, \mathbf{v}_h; \phi_h) - \hat{A}_h(\tilde{\mathbf{u}}_h, \mathbf{v}_h; \phi) \\ &= [\hat{A}(\tilde{\mathbf{u}}_h, \mathbf{v}_h; \phi_h) - \hat{A}(\tilde{\mathbf{u}}_h, \mathbf{v}_h; \phi)] + \sum_{K \in \mathcal{T}_h} \int_{\partial K} (\mu(\phi_h) - \mu(\phi)) (\mathcal{P}^\# \mathbf{v}_h - \mathbf{v}_h) \boldsymbol{\epsilon}(\tilde{\mathbf{u}}_h) \cdot \mathbf{n} \, ds \\ &\quad + \sum_{\sigma \in \mathcal{E}_h} \int_{\sigma} \{(\mu(\phi_h) - \mu(\phi)) \boldsymbol{\epsilon}(\tilde{\mathbf{u}}_h) \mathbf{n}\}_{\sigma} \cdot [\mathcal{P}^\# \mathbf{v}_h]_{\sigma} \, ds + \sum_{\sigma \in \mathcal{E}_h} \int_{\sigma} \{(\mu(\phi_h) - \mu(\phi)) \boldsymbol{\epsilon}(\mathbf{v}_h) \mathbf{n}\}_{\sigma} \cdot [\mathcal{P}^\# \tilde{\mathbf{u}}_h]_{\sigma} \, ds \\ &\quad + \sum_{K \in \mathcal{T}_h} \int_K (\nabla \cdot \mu(\phi_h) - \nabla \cdot \mu(\phi)) \boldsymbol{\epsilon}(\tilde{\mathbf{u}}_h) \cdot (\mathbf{v}_h - \mathcal{P}^\# \mathbf{v}_h) \, dx \\ &=: J_1 + J_2 + J_3 + J_4 + J_5. \end{aligned} \quad (4.25)$$

Employing the definition of $\hat{A}(\cdot, \cdot; \cdot)$, (4.21), the Lipschitz continuity of μ and the Cauchy–Schwarz inequality, we have the following bound for J_1 :

$$|J_1| \leq C \|\phi - \phi_h\|_{0,\Omega} \|\mathbf{v}_h\|_h.$$

In order to bound J_2 , first we note that by using Cauchy–Schwarz inequality, (4.21), the trace inequality (4.3), and (3.4)

$$\begin{aligned} &\left| \int_{\partial K} (\mu(\phi_h) - \mu(\phi)) (\mathcal{P}^\# \mathbf{v}_h - \mathbf{v}_h) \boldsymbol{\epsilon}(\tilde{\mathbf{u}}_h) : \mathbf{n} \, ds \right| \\ &\leq C \left(h_K^{-1/2} \|\phi - \phi_h\|_{0,K} + h_K^{1/2} \|\nabla(\phi - \phi_h)\|_{0,K} \right) h_K^{-1/2} \|\mathcal{P}^\# \mathbf{v}_h - \mathbf{v}_h\|_{0,K} \\ &\leq C (\|\phi - \phi_h\|_{0,K} + h_K \|\nabla(\phi - \phi_h)\|_{0,K}) |\mathbf{v}_h|_{1,K}. \end{aligned}$$

Summing over all triangles and using definitions of the mesh dependent norms $\|\cdot\|_h$ and $\|\cdot\|_h$, we get

$$|J_2| \leq C (\|\phi - \phi_h\|_{0,\Omega} + h \|\phi - \phi_h\|_h) \|\mathbf{v}_h\|_h.$$

Similarly, to bound J_3 again an application of Cauchy–Schwarz inequality, (4.21), and the trace inequality (4.3) yield

$$\begin{aligned} &\left| \int_{\sigma} \{(\mu(\phi_h) - \mu(\phi)) \boldsymbol{\epsilon}(\tilde{\mathbf{u}}_h) \mathbf{n}\}_{\sigma} \cdot [\mathcal{P}^\# \mathbf{v}_h]_{\sigma} \, ds \right| \\ &\leq Ch_{\sigma}^{1/2} \left(h_K^{-1/2} \|\phi - \phi_h\|_{0,K} + h_K^{1/2} \|\nabla(\phi - \phi_h)\|_{0,K} \right) \frac{1}{h_{\sigma}^{1/2}} \|[\mathcal{P}^\# \mathbf{v}_h]_{\sigma}\|_{0,\sigma}. \end{aligned}$$

Repeating the same arguments used in the derivation of (4.14) and definition of $\mathcal{P}^\#$, we have the following inequality $\forall \mathbf{v}_h \in \mathcal{V}(h)$ for $d = 2$, i.e., $\delta = 1$:

$$\frac{1}{h_{\sigma}^{1/2}} \|[\mathcal{P}^\# \mathbf{v}_h]_{\sigma}\|_{0,\sigma} \leq \left(\frac{1}{h_{\sigma}} \int_{\sigma} \|\mathbf{v}_h\|_{\sigma}^2 \, ds \right)^{1/2}. \quad (4.26)$$

Using (4.26), we obtain

$$\begin{aligned} & \left| \int_{\sigma} \{(\mu(\phi_h) - \mu(\phi)) \boldsymbol{\varepsilon}(\tilde{\mathbf{u}}_h) \mathbf{n}\}_{\sigma} \cdot [\![\mathcal{P}^{\#} \mathbf{v}_h]\!]_{\sigma} \, ds \right| \\ & \leq C (\|\phi - \phi_h\|_{0,K} + h_K \|\nabla(\phi - \phi_h)\|_{0,K}) \left(\frac{1}{h_{\sigma}} \int_{\sigma} [\![\mathbf{v}_h]\!]_{\sigma}^2 \, ds \right)^{1/2}. \end{aligned}$$

Now summing over all the edges and using definitions of $\|\cdot\|_h$ and $\|\cdot\|_h$, we have

$$|J_3| \leq C (\|\phi - \phi_h\|_{0,\Omega} + h \|\phi - \phi_h\|_h) \|\mathbf{v}_h\|_h. \quad (4.27)$$

To bound J_4 , first we note that (3.5) implies $[\![\mathcal{P}^{\#} \tilde{\mathbf{u}}_h]\!]_{\sigma} = [\![\mathcal{P}^{\#}(\tilde{\mathbf{u}}_h - \mathbf{u})]\!]_{\sigma}$. Now, a repeated application of the trace inequality (4.3), the one dimensional version (for $d = 2$, the edge σ can be considered as a one-dimensional object) of inverse inequality (4.1) and (4.26) together with fact that \mathbf{v}_h is linear and $\mathcal{P}^{\#}(\cdot)$ is constant on triangle K yields

$$\begin{aligned} & \int_{\sigma} \{(\mu(\phi_h) - \mu(\phi)) \boldsymbol{\varepsilon}(\mathbf{v}_h) \mathbf{n}\}_{\sigma} \cdot [\![\mathcal{P}^{\#} \tilde{\mathbf{u}}_h]\!]_{\sigma} \, ds \leq \|\boldsymbol{\varepsilon}(\mathbf{v}_h)\|_{\infty,\sigma} \|\phi - \phi_h\|_{0,\sigma} \|[\![\mathcal{P}^{\#}(\tilde{\mathbf{u}}_h - \mathbf{u})]\!]_{\sigma}\|_{0,\sigma} \\ & \leq C \|\boldsymbol{\varepsilon}(\mathbf{v}_h)\|_{0,\sigma} \left(h_K^{-1/2} \|\phi - \phi_h\|_{0,K} + h_K^{1/2} \|\nabla(\phi - \phi_h)\|_{0,K} \right) \frac{1}{h_{\sigma}^{1/2}} \|[\![\mathcal{P}^{\#}(\tilde{\mathbf{u}}_h - \mathbf{u})]\!]_{\sigma}\|_{0,\sigma} \\ & \leq C h_K^{-1} \|\boldsymbol{\varepsilon}(\mathbf{v}_h)\|_{0,K} (\|\phi - \phi_h\|_{0,K} + h_K \|\nabla(\phi - \phi_h)\|_{0,K}) \left(\frac{1}{h_{\sigma}} \int_{\sigma} [\![\mathcal{P}^{\#}(\tilde{\mathbf{u}}_h - \mathbf{u})]\!]_{\sigma}^2 \, ds \right)^{1/2}. \end{aligned}$$

Summing over all edges and using the definitions of $\|\cdot\|_h$ and $\|\cdot\|_h$ together with (4.20), we may write

$$|J_4| \leq C (\|\phi - \phi_h\|_{0,\Omega} + h \|\phi - \phi_h\|_h) \|\mathbf{v}_h\|_h. \quad (4.28)$$

For J_5 , first we note that

$$\nabla \cdot \mu(\phi_h) - \nabla \cdot \mu(\phi) = \mu'(\phi_h)(\nabla \phi_h - \nabla \phi) + \nabla \phi (\mu'(\phi_h) - \mu'(\phi)).$$

Now using the Lipschitz continuity and boundedness of μ' and similar arguments used in the bound for J_1 , the following bound for J_5 can be obtained easily:

$$|J_5| \leq Ch (\|\phi - \phi_h\|_{0,\Omega} + h \|\phi - \phi_h\|_h) \|\mathbf{v}_h\|_h.$$

Combining all derived bounds for J_1, \dots, J_5 in (4.25), we have

$$|\hat{A}_h(\tilde{\mathbf{u}}_h, \mathbf{v}_h; \phi_h) - \hat{A}_h(\tilde{\mathbf{u}}_h, \mathbf{v}_h; \phi)| \leq C (\|\phi - \phi_h\|_{0,\Omega} + h \|\phi - \phi_h\|_h) \|\mathbf{v}_h\|_h. \quad (4.29)$$

For all $\mathbf{v}_h \in \mathcal{V}_h$, the following has been shown in Lemma 4.3 of [54]

$$\|\mathbf{v}_h\|_{0,\Omega}^2 \leq C \left[\sum_{K \in \mathcal{T}_h} |\mathbf{v}_h|_{1,K}^2 + \sum_{\sigma \in \mathcal{E}_h} [\![\mathcal{P}^{\#} \mathbf{v}_h]\!]_{\sigma}^2 + \sum_{K \in \mathcal{T}_h} h_K^2 |\mathbf{v}_h|_{2,K}^2 \right].$$

As a consequence of the bound $[\![\mathcal{P}^{\#} \mathbf{v}_h]\!]_{\sigma}^2 \leq \frac{1}{h_{\sigma}} \int_{\sigma} [\![\mathbf{v}_h]\!]_{\sigma}^2 \forall \mathbf{v}_h \in \mathcal{V}_h$ (see (4.26)), an application of (3.12) yields

$$\|\mathbf{v}_h\|_{0,\Omega} \leq C \|\mathbf{v}_h\|_h \quad \forall \mathbf{v}_h \in \mathcal{V}_h. \quad (4.30)$$

Hence, in view of the definition of $d(\cdot, \mathcal{P}^{\#}\cdot)$ together with (3.7) and (4.30), we obtain

$$|d(\phi, \mathcal{P}^{\#} \mathbf{v}_h) - d(\phi_h, \mathcal{P}^{\#} \mathbf{v}_h)| \leq C \|\phi - \phi_h\|_{0,\Omega} \|\mathbf{v}_h\|_h. \quad (4.31)$$

Now, choosing $\mathbf{v}_h = \tilde{\mathbf{u}}_h - \mathbf{u}_h$ in (4.24) and using (3.15), (4.23), and (4.5), i.e., the coercivity of \hat{A}_h together with (4.29) and (4.31), we obtain the following bound for $\tilde{\mathbf{u}}_h - \mathbf{u}_h$:

$$\|\tilde{\mathbf{u}}_h - \mathbf{u}_h\|_h \leq C (\|\phi - \phi_h\|_{0,\Omega} + h \|\phi - \phi_h\|_h). \quad (4.32)$$

In order to find a bound for $\tilde{p}_h - p_h$, we again choose $\mathbf{v}_h = \tilde{\mathbf{u}}_h - \mathbf{u}_h$ in (4.24) and employ (4.29), (4.31), (4.5) and (3.15) to obtain

$$b_h(\tilde{\mathbf{u}}_h - \mathbf{u}_h, \tilde{p}_h - p_h) \leq C (\|\phi - \phi_h\|_{0,\Omega} + h \|\phi - \phi_h\|_h) \|\tilde{\mathbf{u}}_h - \mathbf{u}_h\|_h.$$

By an application of the inf-sup condition given in (4.6) and using (4.32), we arrive at

$$\|\tilde{p}_h - p_h\|_{0,\Omega} \leq C (\|\phi - \phi_h\|_{0,\Omega} + h \|\phi - \phi_h\|_h).$$

The L^2 -norm estimate of $\tilde{\mathbf{u}}_h - \mathbf{u}_h$ follows from $\|\mathbf{v}_h\|_{0,\Omega} \leq C \|\mathbf{v}_h\|_h$ for all $\mathbf{v}_h \in \mathcal{V}_h$, and after employing (4.19) and (4.20), we obtain the desired result. \square

4.3. Error estimates for the concentration field

We decompose the error in $\phi - \phi_h$ as

$$\phi - \phi_h = \eta + \theta, \quad \eta := \phi - R_h\phi, \quad \theta := R_h\phi - \phi_h, \quad (4.33)$$

where $R_h : H^1(\Omega) \rightarrow \mathcal{S}_h$ is the elliptic projection defined as

$$B_h(\phi - R_h\phi, \varphi_h; \phi) = 0 \quad \forall \varphi_h \in \mathcal{S}_h. \quad (4.34)$$

Here, the bilinear form $B_h(\cdot, \cdot; \cdot)$ is same as defined in Section 4.1. Now first we derive error estimates for the projection operator R_h in $\|\cdot\|_h$ and $\|\cdot\|_{0,\Omega}$ norms. We would like to mention that the arguments used for deriving these estimates are quite standard, therefore, for the sake of completeness, we provide the outlines of the proof of the following lemma which deals with an estimate of $\phi - R_h\phi$ in $\|\cdot\|_h$ and $\|\cdot\|_{0,\Omega}$ norms:

Lemma 4.3. *There exists a positive constant C independent of h such that*

$$\|\phi - R_h\phi\|_h \leq Ch\|\phi\|_{2,\Omega}, \quad (4.35)$$

$$\|\phi - R_h\phi\|_{0,\Omega} \leq C(\phi, f, \mathbf{u}) h^2. \quad (4.36)$$

Proof. Let us write $\phi - R_h\phi = \phi - I_h\phi + I_h\phi - R_h\phi$, where $I_h\phi$ denotes the interpolant of ϕ which satisfies the following approximation properties:

$$|\phi - I_h\phi|_{s,K} \leq Ch^{2-s}\|\phi\|_{2,K} \quad \forall K \in \mathcal{T}_h \text{ and } s = 0, 1. \quad (4.37)$$

For a given ϕ , using (3.13), trace inequalities (4.3), Cauchy–Schwarz inequality, we see that $B_h(\cdot, \cdot; \phi)$ is bounded in the following sense (for details, see Lemma 2.4 in [29]):

$$|B_h(\psi, \varphi; \phi)| \leq \|\psi\| \|\varphi\| \quad \forall \psi, \varphi \in \mathcal{S}(h). \quad (4.38)$$

From the definition of $\|\cdot\|$ and (4.37), we obtain

$$\|\phi - I_h\phi\| \leq Ch\|\phi\|_{2,\Omega}.$$

Now using (4.38) and (4.8) together with the definition of R_h , we have

$$\begin{aligned} \beta\|I_h\phi - R_h\phi\|_h^2 &\leq B_h(I_h\phi - R_h\phi, I_h\phi - R_h\phi; \phi) = B_h(I_h\phi - \phi, I_h\phi - R_h\phi; \phi) \\ &\leq C\|\phi - I_h\phi\| \|I_h\phi - R_h\phi\|_h, \end{aligned}$$

and hence,

$$\|I_h\phi - R_h\phi\|_h \leq C\|\phi - I_h\phi\|. \quad (4.39)$$

Now, (4.35) follows after using (4.37) and (4.39). For deriving the L^2 -norm estimates, we first define the following form:

$$\begin{aligned} A_1(\psi_h, \varphi_h; \chi_h) &:= A(\psi_h, \varphi_h; \chi_h) - \sum_{\sigma \in \mathcal{E}_h} \int_{\sigma} \{(\kappa(\chi_h)\nabla\psi_h) \cdot \mathbf{n}\}_{\sigma} \cdot [\![\varphi_h]\!]_{\sigma} \, ds \\ &\quad - \sum_{\sigma \in \mathcal{E}_h} \int_{\sigma} \{\kappa(\chi_h)(\nabla\varphi_h \cdot \mathbf{n})\}_{\sigma} \cdot [\![\psi_h]\!]_{\sigma} \, ds + \sum_{\sigma \in \mathcal{E}_h} \int_{\sigma} \frac{\alpha_c}{h_{\sigma}} [\![\psi_h]\!]_{\sigma} \cdot [\![\varphi_h]\!]_{\sigma} \, ds. \end{aligned}$$

Then first we find the error between $B_h(\cdot, \cdot; \phi)$ and $A_1(\cdot, \cdot; \phi)$. The error on elements (K) as well as on the boundary integrals (∂K) can be computed by following the analysis of [15] and error on the edges (σ) by using the same arguments used in Lemma 3.1 of [29]. Then standard duality arguments can be used to derived optimal error estimates in $\|\phi - R_h\phi\|_{0,\Omega}$ given in (4.36). For detailed proof, we refer to Theorem 4.4 in [15], Lemma 4.4 in [27] and also see [29]. \square

The quasi-uniformity of the mesh implies that there exists a constant C independent of h such that

$$\|\nabla R_h\phi\|_{\infty,K} \leq C, \quad \|\nabla R_h\phi\|_{\infty,\partial K} \leq C, \quad \|R_h\phi\|_{\infty,K} \leq C, \quad \|R_h\phi\|_{\infty,\partial K} \leq C \quad (4.40)$$

(see Theorem 4.7 in [4] and also [39]). Now we provide appropriate estimates for θ (see (4.33)).

Lemma 4.4. *There exists a constant C independent of h such that*

$$\begin{aligned} \|\theta\|_{0,\Omega}^2 &+ \beta_* \int_0^T \|\theta\|_h^2 \, d\tau \\ &\leq C \int_0^t \left(h^4 (\|\mathbf{u}\|_{2,\Omega}^2 + \|p\|_{1,\Omega}^2 + \|\phi g\|_{1,\Omega}^2) + h^2 \|\eta\|_h^2 + \|\eta\|_{0,\Omega}^2 + \|\partial_t \eta\|_{0,\Omega}^2 \right) d\tau. \end{aligned}$$

Proof. First we note that ϕ and $\mathbf{u} = \mathbf{u}^N$ (where we take N large enough in the definition of \mathcal{N} such that $|\mathbf{u}(x)| \leq N$) satisfy

$$\begin{aligned} \langle \partial_t \phi, \mathcal{R}^\sharp \varphi_h \rangle + B_h(\phi, \varphi_h; \phi) &= - \sum_{K \in \mathcal{T}_h} \sum_{j=1}^{d+1} \int_{s_{j+1} b_K s_j} \mathbf{u}^N \cdot \mathbf{n} \phi \mathcal{R}^\sharp \varphi_h \, ds \\ &\quad - \sum_{\sigma \in \mathcal{E}_h} \int_{\sigma} \{\mathbf{u}^N \cdot \mathbf{n} \phi\}_{\sigma} \cdot [\mathcal{R}^\sharp \varphi_h]_{\sigma} \, ds + l_h(\phi; \varphi_h) \quad \forall \varphi_h \in \mathcal{S}_h. \end{aligned} \quad (4.41)$$

Subtracting (4.7) from (4.41), we obtain the following error equation in terms of η and θ :

$$\begin{aligned} & \langle \partial_t \theta, \mathcal{R}^\sharp \varphi_h \rangle + B_h(\theta, \varphi_h; \phi_h) \\ &= [-B_h(\phi, \varphi_h; \phi) - B_h(\eta, \varphi_h; \phi_h) + B_h(\phi, \varphi_h; \phi_h)] + \sum_{K \in \mathcal{T}_h} \sum_{j=1}^{d+1} \int_{s_{j+1} b_K s_j} (\mathbf{u}_h^N - \mathbf{u}^N) \cdot \mathbf{n} \phi \mathcal{R}^\sharp \varphi_h \, ds \\ &\quad + \sum_{K \in \mathcal{T}_h} \sum_{j=1}^{d+1} \int_{s_{j+1} b_K s_j} (\phi_h - \phi) \mathbf{u}_h^N \cdot \mathbf{n} \mathcal{R}^\sharp \varphi_h \, ds + \sum_{\sigma \in \mathcal{E}_h} \int_{\sigma} \{(\mathbf{u}_h^N - \mathbf{u}^N) \cdot \mathbf{n} \phi\}_{\sigma} \cdot [\mathcal{R}^\sharp \varphi_h]_{\sigma} \, ds \\ &\quad + \sum_{\sigma \in \mathcal{E}_h} \int_{\sigma} \{(\phi_h - \phi) \mathbf{n} \cdot \mathbf{u}_h^N\}_{\sigma} \cdot [\mathcal{R}^\sharp \varphi_h]_{\sigma} \, ds - \langle \partial_t \eta, \mathcal{R}^\sharp \varphi_h \rangle + l_h(\phi - \phi_h; \varphi_h) \\ &=: I_1 + I_2 + I_3 + I_4 + I_5 + I_6 + I_7. \end{aligned} \quad (4.42)$$

Now we estimate I_1, \dots, I_7 one by one. By using (4.34), we have

$$B_h(\phi, \varphi_h; \phi_h) - B_h(\phi, \varphi_h; \phi) - B_h(\eta, \varphi_h; \phi_h) = B_h(R_h \phi, \varphi_h; \phi_h) - B_h(R_h \phi, \varphi_h; \phi),$$

and hence by using the definition of $B_h(\cdot, \cdot; \cdot)$, we have

$$\begin{aligned} B_h(R_h \phi, \varphi_h; \phi_h) - B_h(R_h \phi, \varphi_h; \phi) &= \sum_{K \in \mathcal{T}_h} \sum_{j=1}^{d+1} \int_{s_{j+1} b_K s_j} (\kappa(\phi) - \kappa(\phi_h)) \nabla(R_h \phi) \cdot \mathbf{n} \mathcal{R}^\sharp \varphi_h \, ds \\ &\quad + \sum_{\sigma \in \mathcal{E}_h} \int_{\sigma} \{[\kappa(\phi) - \kappa(\phi_h)] \nabla(R_h \phi)\} \cdot \mathbf{n} \cdot [\mathcal{R}^\sharp \varphi_h]_{\sigma} \, ds \\ &\quad + \sum_{\sigma \in \mathcal{E}_h} \int_{\sigma} \{(\kappa(\phi) - \kappa(\phi_h)) \nabla \varphi_h \cdot \mathbf{n}\}_{\sigma} \cdot [\mathcal{R}^\sharp(R_h \phi)]_{\sigma} \, ds \\ &=: T_1 + T_2 + T_3. \end{aligned}$$

Using (3.13), we rewrite T_1 as

$$\begin{aligned} T_1 &= [A(R_h \phi, \varphi_h; \phi_h) - A(R_h \phi, \varphi_h; \phi)] + \sum_{K \in \mathcal{T}_h} \int_{\partial K} (\kappa(\phi_h) - \kappa(\phi)) \nabla(R_h \phi) \cdot \mathbf{n} (\mathcal{R}^\sharp \varphi_h - \varphi_h) \, ds \\ &\quad + \sum_{K \in \mathcal{T}_h} \int_K \nabla[(\kappa(\phi_h) - \kappa(\phi)) \nabla(R_h \phi)](\varphi_h - \mathcal{R}^\sharp \varphi_h) \, dx =: T_1^1 + T_1^2 + T_1^3. \end{aligned}$$

Employing the definition of $A(\cdot, \cdot; \cdot)$ together with Cauchy–Schwarz inequality and (4.40), we obtain

$$|T_1^1| \leq C \|\phi - \phi_h\|_{0,\Omega} \|\phi_h\|_{H^1}.$$

Again, an application of (4.40) together with trace inequality (4.3) and (3.4) yields

$$\begin{aligned} & \int_{\partial K} (\kappa(\phi_h) - \kappa(\phi)) \nabla(R_h \phi) \cdot \mathbf{n} (\mathcal{R}^\sharp \varphi_h - \varphi_h) \, ds \\ & \leq C \left(h_K^{-1/2} \|\phi - \phi_h\|_{0,K} + h_K^{1/2} \|\nabla(\phi - \phi_h)\|_{0,K} \right) \\ & \quad \times \left(h_K^{-1/2} \|\mathcal{R}^\sharp \varphi_h - \varphi_h\|_{0,K} + h_K^{1/2} \|\nabla(\mathcal{R}^\sharp \varphi_h - \varphi_h)\|_{0,K} \right) \\ & \leq C (\|\phi - \phi_h\|_{0,K} + h_K \|\nabla(\phi - \phi_h)\|_{0,K}) \|\nabla \varphi_h\|_{0,K}. \end{aligned}$$

Then, summation over all triangles gives

$$|T_1^2| \leq C (\|\phi - \phi_h\|_{0,\Omega} + h \|\phi - \phi_h\|_h) \|\varphi_h\|_h.$$

To estimate T_1^3 , we argue as follows: Since $R_h\phi$ is linear on each triangle, we note that

$$\begin{aligned} \nabla \cdot [(\kappa(\phi_h) - \kappa(\phi)) \nabla R_h\phi] &= (\nabla \kappa(\phi_h) - \nabla \kappa(\phi)) \cdot \nabla (R_h\phi) = (\kappa'(\phi_h) \nabla \phi_h - \kappa'(\phi) \nabla \phi) \cdot \nabla (R_h\phi) \\ &= [\kappa'(\phi_h) (\nabla \phi_h - \nabla \phi) + \nabla \phi (\kappa'(\phi_h) - \kappa'(\phi))] \cdot \nabla (R_h\phi), \end{aligned}$$

and therefore, by assuming that κ' is Lipschitz continuous and using Cauchy–Schwarz inequality, (3.4), (4.40), (2.2), we have

$$|T_1^3| \leq C(\gamma_3)h (\|\phi - \phi_h\|_{0,\Omega} + \|\phi - \phi_h\|_h) \|\varphi_h\|_h.$$

Combining the estimates of T_1^1 , T_1^2 and T_1^3 , we obtain the following bound for T_1 :

$$|T_1| \leq C (\|\phi - \phi_h\|_{0,\Omega} + h \|\phi - \phi_h\|_h) \|\varphi_h\|_h.$$

For T_2 , we use the same arguments used in the bound for J_3 given in (4.27) and (4.40) to obtain

$$|T_2| \leq C (\|\phi - \phi_h\|_{0,\Omega} + h \|\phi - \phi_h\|_h) \|\varphi_h\|_h.$$

To bound T_3 , first we note that from (3.5), we have $\llbracket \mathcal{R}^\sharp(R_h\phi) \rrbracket_\sigma = \llbracket \mathcal{R}^\sharp(R_h\phi - \phi) \rrbracket_\sigma$. Now following the same techniques used in the accomplishment of (4.28), where (4.35) is used in place of (4.20), we immediately conclude that

$$|T_3| \leq C (\|\phi - \phi_h\|_{0,\Omega} + h \|\phi - \phi_h\|_h) \|\varphi_h\|_h,$$

and hence,

$$|I_1| \leq C (\|\phi - \phi_h\|_{0,\Omega} + h \|\phi - \phi_h\|_h) \|\varphi_h\|_h.$$

Using (4.4) and the uniform boundedness of \mathbf{u}_h^N , we have from (4.13)

$$|I_2|, |I_3| \leq C (\|\mathbf{u} - \mathbf{u}_h\|_{0,\Omega} + h \|\mathbf{u} - \mathbf{u}_h\|_h) \|\varphi_h\|_h.$$

Again using the same techniques which were used to bound J_3 together with (4.4) and $\mathbf{u}_h^N \in L^\infty(\Omega)$, we easily obtain the following bounds for I_4 and I_5

$$|I_4|, |I_5| \leq C (\|\mathbf{u} - \mathbf{u}_h\|_{0,\Omega} + h \|\mathbf{u} - \mathbf{u}_h\|_h) \|\varphi_h\|_h.$$

An application of the Cauchy–Schwarz inequality together with L^2 stability of \mathcal{R}^\sharp , i.e., (3.7) yields

$$|I_6| \leq C \|\partial_t \eta\|_{0,\Omega} \|\varphi_h\|_{0,\Omega}.$$

With the help of (4.16) and the assumption that f is Lipschitz continuous, we have

$$|I_7| \leq C (\|\phi - \phi_h\| + h \|\phi - \phi_h\|_h) \|\varphi_h\|_h.$$

Choosing $\varphi_h = \theta$, substituting all the estimates of I_1, \dots, I_7 into (4.42) and using Lemma 4.2 together with (4.8), Young's inequality ($ab \leq \frac{\xi}{2}a^2 + \frac{1}{2\xi}b^2$ for all $a, b \in \mathbb{R}$ and $\xi > 0$), and classical “kick-back” arguments (i.e. adding an existing term multiplied by a small constant, only to be conveniently eliminated afterwards), we arrive at

$$\begin{aligned} &(\partial_t \theta, \mathcal{R}^\sharp \theta) + (\beta - \xi) \|\theta\|_h^2 \\ &\leq C \left(\|\theta\|_{0,\Omega}^2 + h^4 (\|\mathbf{u}\|_{2,\Omega}^2 + \|p\|_{1,\Omega}^2 + \|\phi g\|_{1,\Omega}^2) + h^2 \|\eta\|_h^2 + \|\eta\|_{0,\Omega}^2 + \|\partial_t \eta\|_{0,\Omega}^2 \right). \end{aligned} \quad (4.43)$$

Let us define the norm $\|\varphi_h\|_1 := (\varphi_h, \mathcal{R}^\sharp \varphi_h)$. Note that \mathcal{R}^\sharp satisfy the following properties, see [27, pp. 1365]:

$$(\varphi_h, \mathcal{R}^\sharp \psi_h) = (\psi_h, \mathcal{R}^\sharp \varphi_h) \quad \forall \varphi_h, \psi_h \in \mathcal{S}_h. \quad (4.44)$$

Moreover, $\|\cdot\|_1$ and $\|\cdot\|_{0,\Omega}$ are equivalent, i.e., there exist $C_1 > 0$ and $C_2 > 0$ independent of h such that

$$C_1 \|\psi_h\|_{0,\Omega} \leq \|\psi_h\|_1 \leq C_2 \|\psi_h\|_{0,\Omega} \quad \forall \psi_h \in \mathcal{S}_h. \quad (4.45)$$

Employing (4.44), we obtain from (4.43)

$$\frac{1}{2} \frac{d}{dt} (\theta, \mathcal{R}^\sharp \theta) + \beta_* \|\theta\|_h^2 \leq C \left(\|\theta\|_{0,\Omega}^2 + \|\mathbf{u} - \mathbf{u}_h\|_{0,\Omega}^2 + h^2 \|\mathbf{u} - \mathbf{u}_h\|_h^2 + h^2 \|\eta\|_h^2 + \|\eta\|_{0,\Omega}^2 + \|\partial_t \eta\|_{0,\Omega}^2 \right).$$

We proceed to choose $\phi_h(0) = R_h\phi(0)$, which implies that $\theta(0) = 0$. Now, an application of Gronwall's inequity together with (4.45) enables us to write

$$\|\theta\|_{0,\Omega}^2 + \beta_* \int_0^T \|\theta\|_h^2 d\tau \leq C \int_0^T \left(h^4 (\|\mathbf{u}\|_{2,\Omega}^2 + \|p\|_{1,\Omega}^2 + \|\phi g\|_{1,\Omega}^2) + h^2 \|\eta\|_h^2 + \|\eta\|_{0,\Omega}^2 + \|\partial_t \eta\|_{0,\Omega}^2 \right) d\tau,$$

which completes the proof. \square

Table 1

Example 1: Convergence test against an analytical solution employing DFVE approximations of concentration, velocity and pressure computed on a sequence of uniformly refined triangulations of the unit square.

h	$e_0(\phi)$	rate	$e_h(\phi)$	rate	$e_0(\mathbf{u})$	rate	$e_h(\mathbf{u})$	rate	$e_0(p)$	rate
0.28284	0.000417	–	0.01468	–	0.005051	–	0.08445	–	0.09067	–
0.14142	9.985e–5	2.0643	0.00751	0.9657	0.001362	1.8900	0.04345	0.9586	0.04526	1.0021
0.07071	2.443e–5	2.0311	0.00379	0.9866	0.000352	1.9493	0.02202	0.9805	0.02259	1.0026
0.03535	6.124e–6	1.9988	0.00190	0.9950	8.971e–5	1.9760	0.01108	0.9906	0.01128	1.0014
0.01767	1.742e–6	1.9967	0.00095	1.0002	2.260e–5	1.9883	0.00555	0.9954	0.00564	1.0006
0.00883	4.385e–7	1.9682	0.00047	1.0075	5.676e–6	1.9939	0.00278	0.9977	0.00281	1.0002
0.00441	1.097e–7	1.9578	0.00023	1.0093	1.423e–6	1.9955	0.00139	0.9988	0.00140	1.0000
0.00220	2.562e–8	1.9305	0.00012	1.0010	3.671e–7	1.9920	0.00070	0.9995	0.00070	1.0000

Theorem 4.5 (Error estimates). Let $(\phi_h(t), \mathbf{u}_h(t), p_h(t)) \in \mathcal{S}_h \times \mathcal{V}_h \times \mathcal{Q}_h$ be the unique solution of (3.9)–(3.11) and $(\phi(t), \mathbf{u}(t), p(t))$ the unique solution of (2.4) for a fixed time $t < T$. Then, under the assumption that $\phi_h(0) = R_h\phi(0)$, there exists $C > 0$ such that

$$\|\phi(t) - \phi_h(t)\|_{0,\Omega} \leq C(\phi, \phi_t, \mathbf{f}, \mathbf{u}, p, g) h^2, \quad (4.46)$$

$$\int_0^T \|\phi - \phi_h\|_h d\tau \leq C(\phi, \phi_t, \mathbf{f}, \mathbf{u}, p, g) h, \quad (4.47)$$

$$\|\mathbf{u}(t) - \mathbf{u}_h(t)\|_{0,\Omega} \leq C(\phi, \phi_t, \mathbf{f}, \mathbf{u}, p, g) h^2, \quad (4.48)$$

$$\|\mathbf{u}(t) - \mathbf{u}_h(t)\|_h + \|p(t) - p_h(t)\|_{0,\Omega} \leq C(\phi, \phi_t, \mathbf{f}, \mathbf{u}, p, g) h. \quad (4.49)$$

Proof. (4.46) and (4.47) follow by combining the estimates given in (4.35), (4.36) and Lemma 4.4 whereas (4.48) and (4.49) directly follow from (4.46), (4.47) and Lemma 4.2. \square

5. Numerical examples

We now present a series of numerical tests confirming the convergence rates predicted in Section 4 and simulating some interesting scenarios from the applicative viewpoint. For consistency with the analysis in the previous sections, we do not address here the convergence of the time discretization and we simply employ a first order backward Euler formula with a fixed time step. The resulting system of nonlinear equations (the fully discrete counterpart of (3.9)–(3.11)) is solved via the Newton–Raphson method with a tolerance of 10^{-8} for the energy norm of the residual, and, given the moderate size of the associated linear systems, these are solved with the unsymmetric-pattern multi-frontal direct solver for sparse systems, a routine which is part of the UMFPACK library. The specific form of the linearized problem is postponed to Appendix A. The penalty parameters are set as $\alpha_c = 10^{-6}$, $\alpha_d = 10^3$.

5.1. Example 1: experimental order of convergence against a manufactured exact solution

In Example 1 the ingredients of (1.1) are chosen in such a way that an exact solution is known. To this end, we choose $\kappa(\phi) = \phi^3(1 - \phi/2)^2$, $\mu(\phi) = (1 - \phi/2)^{-2}$, and consider the non-homogeneous problem resulting from adding a non-zero datum \mathbf{j} to the right-hand side of (1.1b). The spatial domain is $\Omega = (0, 1)^2$, and the source terms f (which replaces $\nabla \cdot \mathbf{f}(\phi)$) and \mathbf{j} are constructed so that its solution is given by the smooth functions

$$\mathbf{u}(x, y, t) = \begin{pmatrix} \sin(\pi x) \cos(\pi y) \sin(t) \\ -\cos(\pi x) \sin(\pi y) \sin(t) \end{pmatrix}, \quad p(x, y, t) = (x^2 + y^2 - 2/3) \cos(t),$$

$$\phi(x, y, t) = \sin(\pi x) \sin(\pi y) \sin(t).$$

Dirichlet boundary and initial conditions are chosen according to these solutions. We first apply the proposed FVE method on meshes obtained by successive subdivision of Ω into quasi-uniform triangulations \mathcal{T}_h of meshsizes $h = \frac{1}{5}2^{-k}$, with $0 \leq k \leq 6$. The system is evolved with a fixed time step $\Delta t = 0.01$ until $T = 1$ and the approximate solutions obtained on the refinement level $k = 6$ are displayed in Fig. 2.

Individual errors in different norms are defined as

$$e_0(\mathbf{u}) = \left\| \mathbf{u}(t^{N_T}) - \mathbf{u}_h(t^{N_T}) \right\|_{0,\Omega}, \quad e_h(\mathbf{u}) = \left\| \mathbf{u}(t^{N_T}) - \mathbf{u}_h(t^{N_T}) \right\|_h,$$

$$e_0(p) = \left\| p(t^{N_T}) - p_h(t^{N_T}) \right\|_{0,\Omega}, \quad e_h(\phi) = \left\| \phi(t^{N_T}) - \phi_h(t^{N_T}) \right\|_h, \quad e_0(\phi) = \left\| \phi(t^{N_T}) - \phi_h(t^{N_T}) \right\|_{0,\Omega}.$$

As expected, we observe in Table 1 a convergence of approximate order h^2 for $e_0(\mathbf{u}(t))$ and $e_0(\phi(t))$, and order h for the other spatial errors in their respective norms. An experimental convergence of order Δt (not shown here) has also been

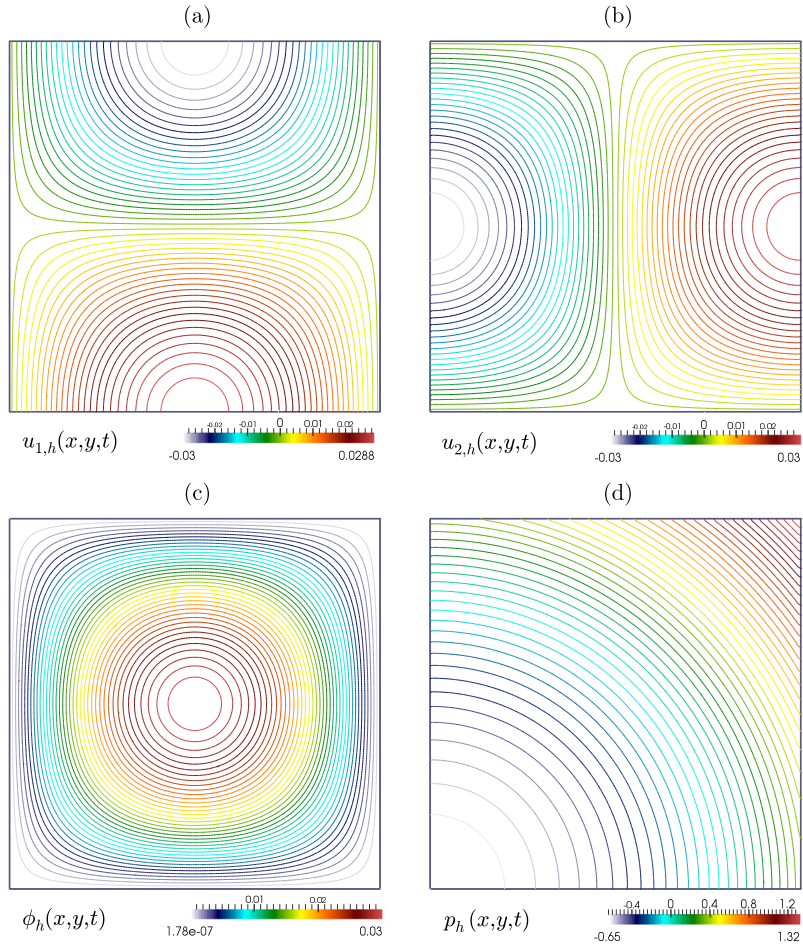


Fig. 2. Example 1: Contour plots of the discontinuous finite volume element approximations of velocity components (top panels), and concentration and pressure fields (bottom panels) at the time instant $t = 1$.

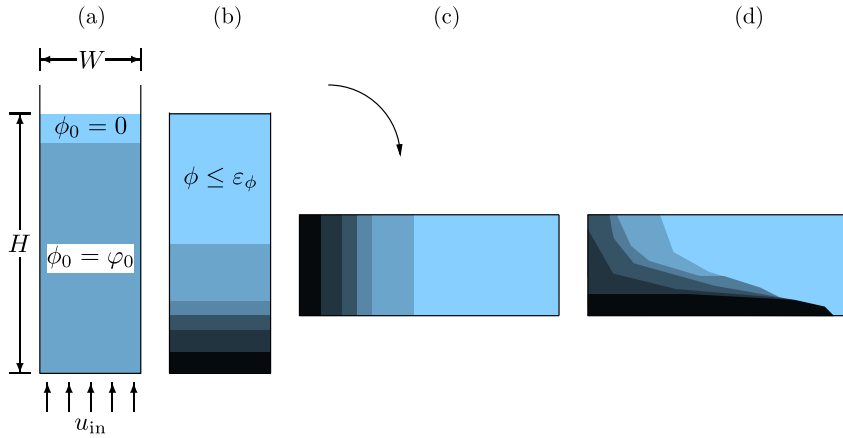


Fig. 3. Example 2: Spreading of a gravity current [45]. (a) Initial state (not to scale). (b) Once the concentration values in the lower half of the vessel are larger than ε_ϕ , the vessel is tilted. (c) Tilted vessel, (d) gravity current.

observed for all variables in the $\ell^\infty(0, t; L^2(\Omega))$ -norm. An average iteration count (through all refinement levels and time steps) of six Newton steps to achieve the imposed tolerance has been evidenced.

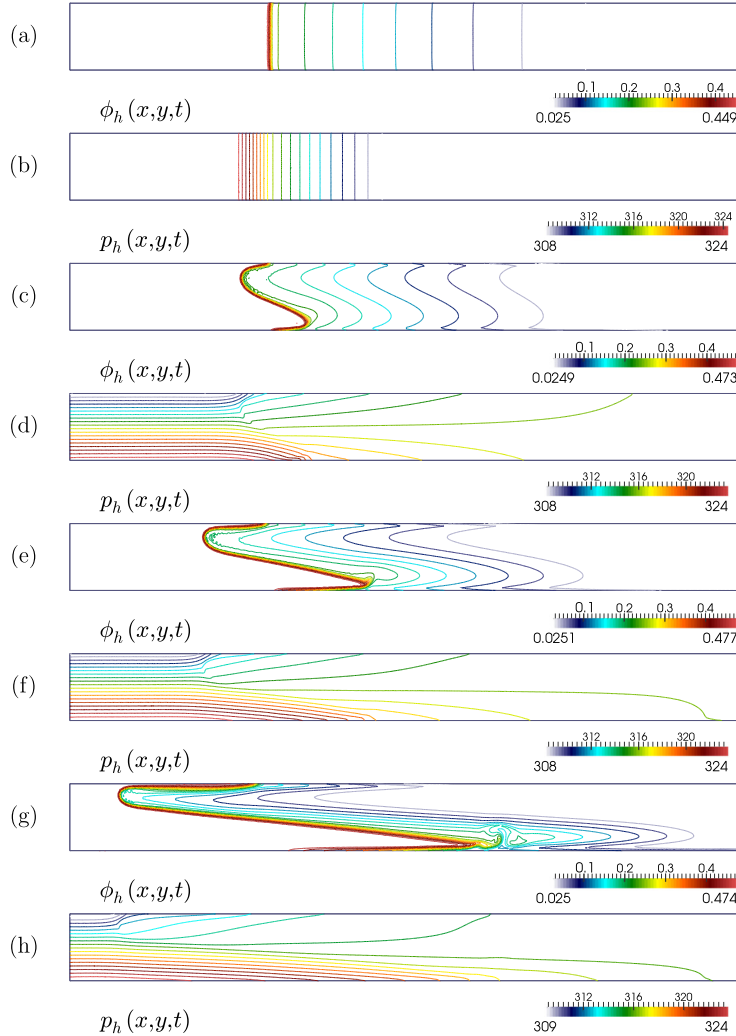


Fig. 4. Example 2: Contour plots of the discontinuous finite volume element approximations of (a), (c), (e), (g) concentrations and (b), (d), (f), (h) pressures at time instants (a), (b) $t = 1000$ s (before tilting at $T^* = 1500$), (c), (d) $t = 4000$, (e), (f) $t = 8000$ and (g), (h) $t = 20000$.

5.2. Example 2: spreading of a suspension gravity current

In this test we are interested in recovering the flow patterns of an experiment carried out in [45]. It consists in a scenario where a rectangular vessel is initially placed vertically, and two separate zones with clear liquid and average concentration are present, and an inflow velocity of normal $\mathbf{u} \cdot \mathbf{n} = u_{\text{in}}$ is imposed at the inlet, located at the bottom of the domain (see the sketch provided in Fig. 3). Next, the system evolves and from $t > 0$ to $t = T^*$ three separate zones of clear liquid, suspension at intermediate concentration, and packed sediment are present, and the inflow velocity is still imposed at the inlet. Suddenly, at $t = T^*$ (which corresponds to a time when a jamming concentration $\varepsilon_\phi = 0.475$ is attained at the bottom of the vessel), the inflow is stopped and the gravity direction is switched -90 degrees, and from $t = T^*$ to $t = T$, one observes the resulting mixing patterns.

The domain is a rectangle of width $W = 50$ and height $H = 500$, and the initial distribution of the concentration is $\phi_0 = 0.4(H - y)^2/H^2$. Zero-flux boundary conditions are considered for ϕ everywhere and no-slip data for \mathbf{u} on the top, left, and right boundaries. For this problem we do not consider the effect of sediment compression and so we take $\kappa = D_0$. Instead of $\phi\mathbf{g}$, in this case the forcing term acting on the momentum equation is considered as

$$\frac{(\rho_s - \rho_f)\phi}{(1 - \phi)\rho_f + \phi\rho_s}\mathbf{g},$$

and the remaining (adimensional) model parameters are chosen as follows: $\beta = 5$, $\tilde{\phi}_{\text{max}} = 0.6$, $u_{\text{in}} = 1.58 \times 10^{-3}$, $D_0 = 10^{-3}$, $T^* = 1500$, $\rho_f = 2500$, $g = 1.0$, $\Delta\rho = 1300$. A mesh of 51108 primal cells and 25 555 vertices and a timestep of $\Delta t = 0.05$ are employed in the simulations. Fig. 4 shows the concentration profiles and pressure distribution during a

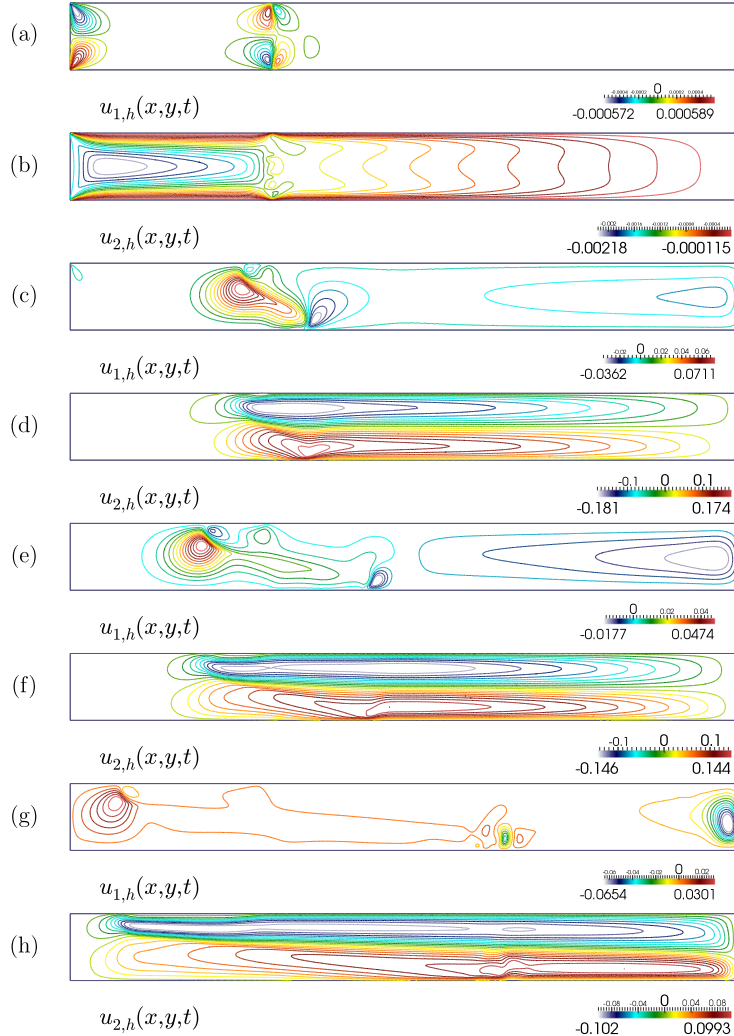


Fig. 5. Example 2: Contour plots of the discontinuous finite volume element approximations of the velocity components (a), (c), (e), (g) u_1 (in x -direction, aligned with the vessel width) and (b), (d), (f), (h) u_2 (in y -direction, aligned with the vessel height) at time instants (a), (b) $t = 1000$ (before tilting at $T^* = 1500$), (c), (d) $t = 4000$, (e), (f) $t = 8000$ and (g), (h) $t = 20000$.

transient simulation (for visualization purposes the tank is rendered already tilted), whereas Fig. 5 depicts contour plots of the associated velocity components.

5.3. Example 3: simulation of an axisymmetric secondary settling tank

We now simulate the sedimentation of a zeolites suspension taking place in a secondary clarifier located in the Eindhoven WWTP [6]. Since the vessel and the expected flow patterns are intrinsically axisymmetric, we can restrict the study to a half cross-section of the tank. The axisymmetric domain is presented in Fig. 6, along with its dimensions and different parts of its boundary. Such a configuration requires some modifications to the continuous and discrete formulations of the model problem, in particular, all differential operators, infinite and finite-dimensional functional spaces need to be accommodated to the axisymmetric case. A summary of these ingredients is collected in Appendix B (cf., e.g., [11] for details).

The meridional domain Ω sketched in Fig. 6 was discretized using an unstructured primal mesh of 96 772 triangular elements and 48 387 vertices. A fixed timestep of $\Delta t = 3$ s was employed and the system was evolved until $T = 120\,000$ s. The suspension fed through Γ_{in} with velocity $\mathbf{u}_{\text{in}} = (0, 0.17)^T$ has a concentration of $\phi_{\text{in}} = 0.08$. The material is removed with a constant velocity $\mathbf{u}_{\text{out}} = (0, -0.0000015)^T$ through Γ_{out} , and a constant pressure profile is imposed at the overflow Γ_{off} . In all remaining parts of the boundary we impose zero-flux boundary conditions for the concentration and, except for the symmetry axis, we set no-slip velocities everywhere on $\partial\Omega$. Other functions and parameters are set as $\sigma_e(\phi) = (\sigma_0 \alpha / \phi_c^\alpha) \phi^{\alpha-1}$, $\sigma_0 = 0.22$ Pa, $\alpha = 5$, $\beta = 2.5$, $\rho_f = 998.2$ kg/m³, $\rho_s = 1750$ kg/m³, $\phi_c = 0.014$, $\dot{\phi}_{\text{max}} = 0.95$, $v_\infty = 0.0028935$ m/s, $g = 9.8$ m/s², and $D_0 = 0.0028935$ m²/s.

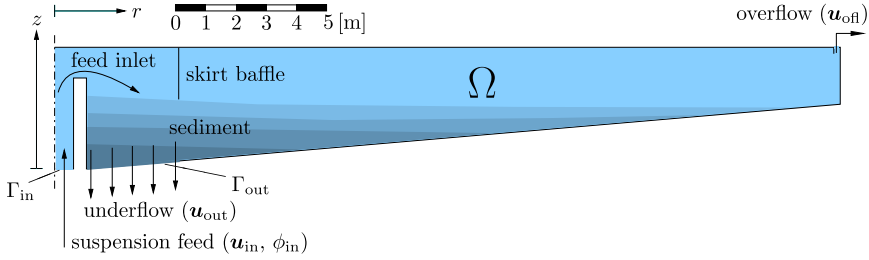


Fig. 6. Example 3: Secondary settling tank [6]. The device has a feed inlet, a radial underflow for the discharge of sediment, and a peripheral overflow. The variables prescribed on the portions Γ_{in} , Γ_{out} and Γ_{ofl} of the boundary of the (r, z) -domain $\Omega \subset \mathbb{R}^2$ are indicated. The device has a radial length and height of 26 m and 4 m, respectively. The inlet, Γ_{in} , is a horizontal disk of radius 0.6 m. The underflow opening corresponds to the zone from $r = 1.05$ m to $r = 4.1$ m of the conical bottom. The overflow channel corresponds to the annulus between $r = 25.8$ m and $r = 26$ m at $z = 4$ m. The skirt baffle is a thin solid wall reaching from $z = 2.3$ m to $z = 4$ m at $r = 4.1$ m.

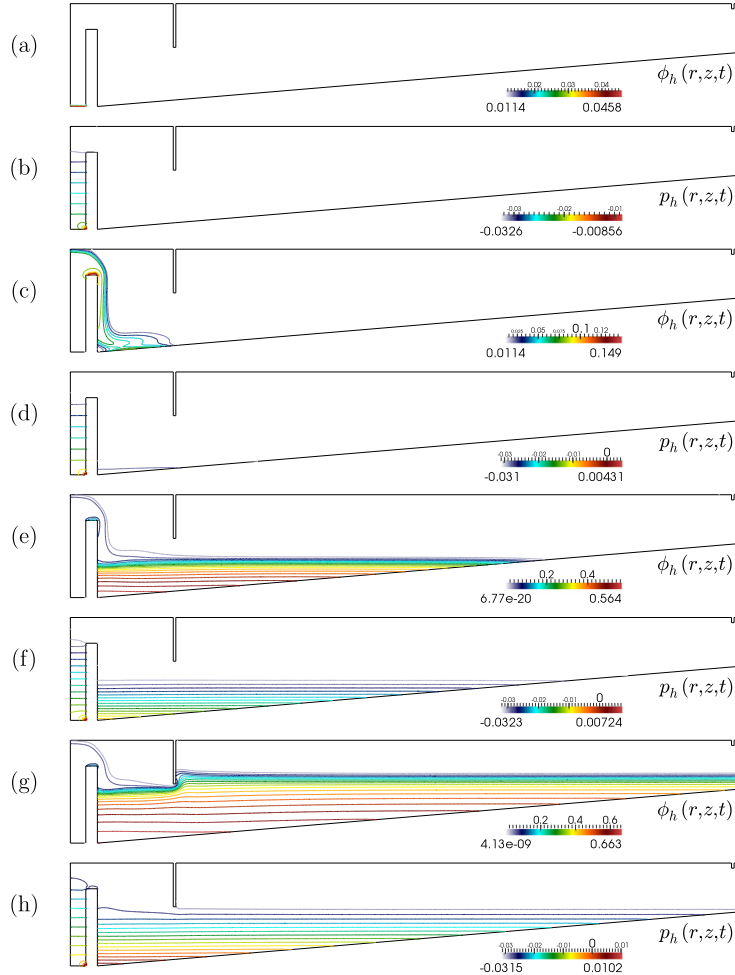


Fig. 7. Example 3: Contour plots of the discontinuous finite volume element approximations of (a), (c), (e), (g) concentration and (b), (d), (f), (h) pressure at time instants (a), (b) $t = 100$ s, (c), (d) $t = 5000$ s, (e), (f) $t = 50000$ s and (g), (h) $t = 100000$ s.

Snapshots of the approximate solutions computed on the axisymmetric domain are presented in Figs. 7 and 8. For visualization purposes, we also depict a rotational extrusion of 330 degrees at the final time 120 000 s in Fig. 9.

5.4. Example 4: settling in an inclined cylinder

The settling rate of solid particles within a tilted vessel is known to be accelerated with respect to that in vertical walls. In our last example we study this phenomenon, commonly known as the Boycott effect [7], where we also test our

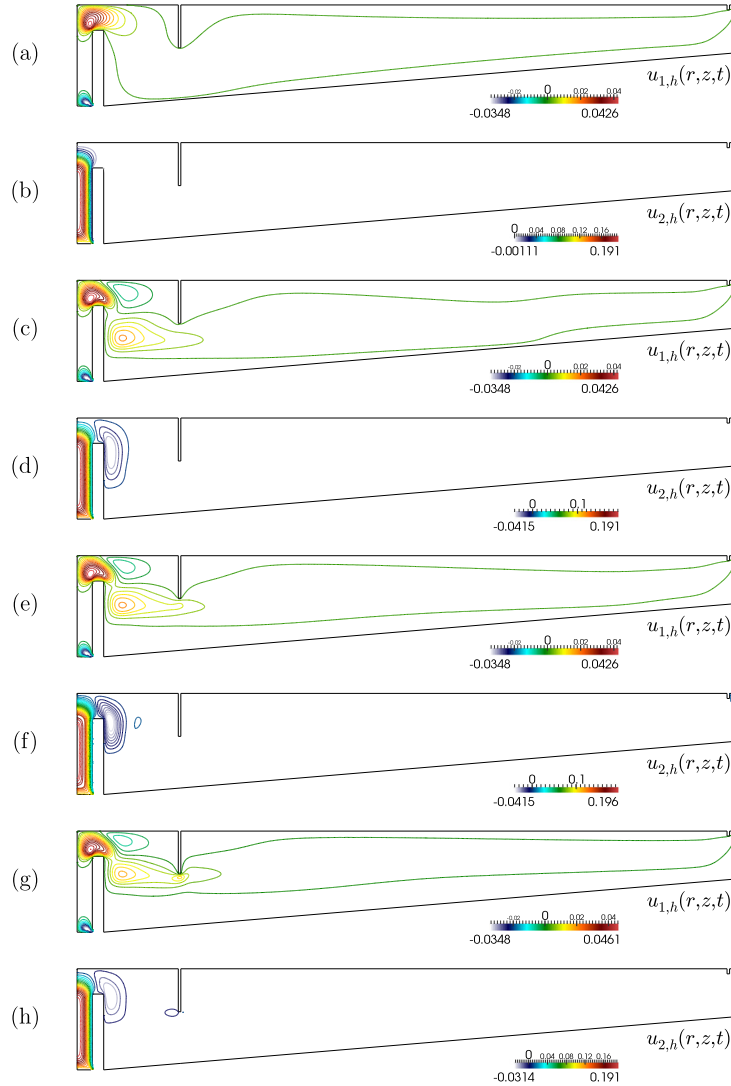


Fig. 8. Example 3: Contour plots of the discontinuous finite volume element approximations of the velocity components (a), (c), (e), (g) u_1 (in radial direction) and (b), (d), (f), (h) u_2 (in vertical direction) at time instants (a), (b) $t = 100$ s, (c), (d) $t = 5000$ s, (e), (f) $t = 50000$ s and (g), (h) $t = 100000$ s.

three-dimensional DFVE implementation. The material behavior and model parameters are assumed as in Example 3, but we take again adimensional units. The computational domain consists of a tilted cylinder of height 8 and radius 2, forming an angle of 45° with the y -axis. The concentration-dependent viscosity is given by (2.3) with $\tilde{\phi}_{\max} = 0.85$ and $\beta = 2$. An unstructured mesh of 48 361 vertices and 267 297 tetrahedral primal elements has been generated to discretize the domain. We employ a timestep of $\Delta t = 0.01$ and evolve the system until $T = 16$. We study the elementary batch-sedimentation case, therefore no-flux boundary conditions for the concentration, and no-slip velocities are set on the whole boundary (see also [43]). Three snapshots of the approximate solutions are displayed in Fig. 10.

6. Concluding remarks

We have presented the numerical analysis of a DFVE method for the numerical approximation of a coupled PDE system governing the sedimentation-consolidation process of solid-liquid suspensions. The proposed numerical scheme was formulated on the basis of a discontinuous piecewise linear approximation of velocity and concentration, and piecewise constant pressure approximation. In general, DFVE methods also possess local conservation properties (hold for classical and mixed finite volume methods) on the dual elements, which are desirable while seeking numerical approximations of the problems following physically conservation laws including mass, momentum, etc. In addition, the size of the dual elements used in these methods is almost half of the size of dual elements used by classical and mixed finite volume methods. The solvability of the nonlinear discrete problem was discussed and *a priori* error estimates for concentration, velocity and pressure in different norms have been established rigorously. A comprehensive set of numerical tests in two and three spatial dimensions

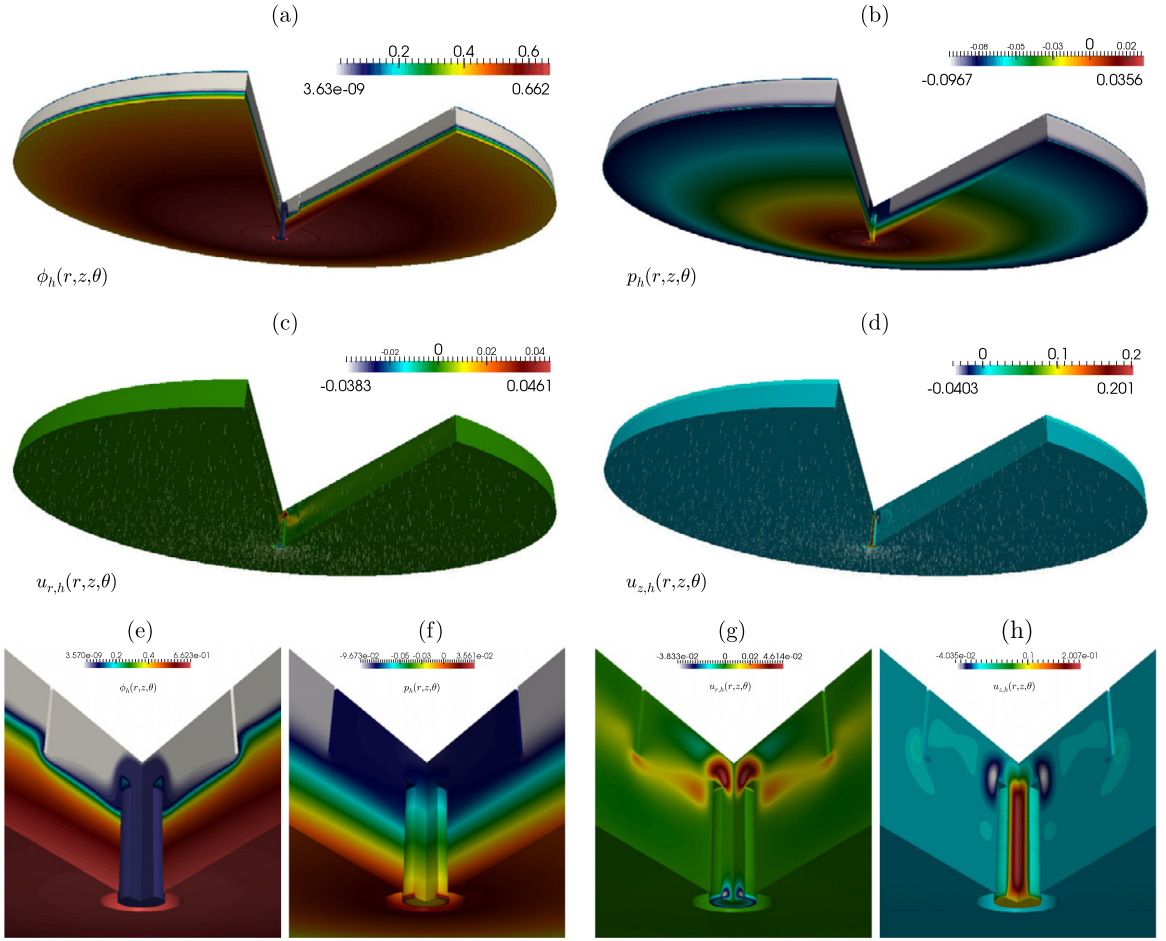


Fig. 9. Example 3: Rotational extrusion of the discontinuous finite volume element approximations of (a) concentration, (b) pressure, (c) radial and (d) vertical velocity components, and zoomed views of the inlet region (e), (f), (g), (h) at time $t = 120\,000$ s.

illustrates the robustness of the proposed method. The applicability of this scheme to the transport–flow coupling arising in other two-phase flow models, such as those of granular-like behavior that are based on similar equations [3,26], is yet to be tested.

It should be noticed, however, that a proof of consistency with continuity (CWC) (exact mass conservation at the discrete level for the concentration equation) is currently not available for the present scheme. Possible remedies include combination with semi-Lagrangian transport schemes, or the so-called explicit flux modification (cf. [35,46]). Mass-lumping flux-correction strategies targeted for CWC enforcement could be also incorporated without much effort (see e.g. [31]). Moreover, monotonicity properties (essential in avoiding spurious oscillations and non-physical concentrations) are not discussed within our theoretical analysis, but our computational experiments along with coercivity and discrete inf-sup conditions satisfied by the formulation may indicate that this property holds. A few contributions have dealt with the construction of monotone finite element methods, under mesh regularity assumptions [8,51] (see also [21] and the references therein). Similar studies could be applied in our case if we perform an operator splitting and study the monotonicity of the DFVE scheme for the concentration equation following the analysis for a continuous FVE approximation of a parabolic problem presented in [20]. Nevertheless, monotonicity of the fully coupled scheme remains a difficult task in view of all involved nonlinearities and will be part of a forthcoming study. In that case, upwind or more sophisticated numerical fluxes should be applied (our current choice obeys primarily to permit straightforward error estimation).

Acknowledgements

The authors would like to thank the referees for their constructive comments and suggestions, which led to a number of improvements to this manuscript. We also thank Elena Torfs (BIOMATH, Ghent University) for providing the geometry and expected flow conditions addressed in Section 5.3. In addition, RB is supported by FONDECYT project 1130154; BASAL project CMM, Universidad de Chile and Centro de Investigación en Ingeniería Matemática (CIMMA), Universidad de Concepción; CONICYT project Anillo ACT1118 (ANANUM); Red Doctoral REDOC.CTA, MINEDUC project UCO1202; and CRHIAM,

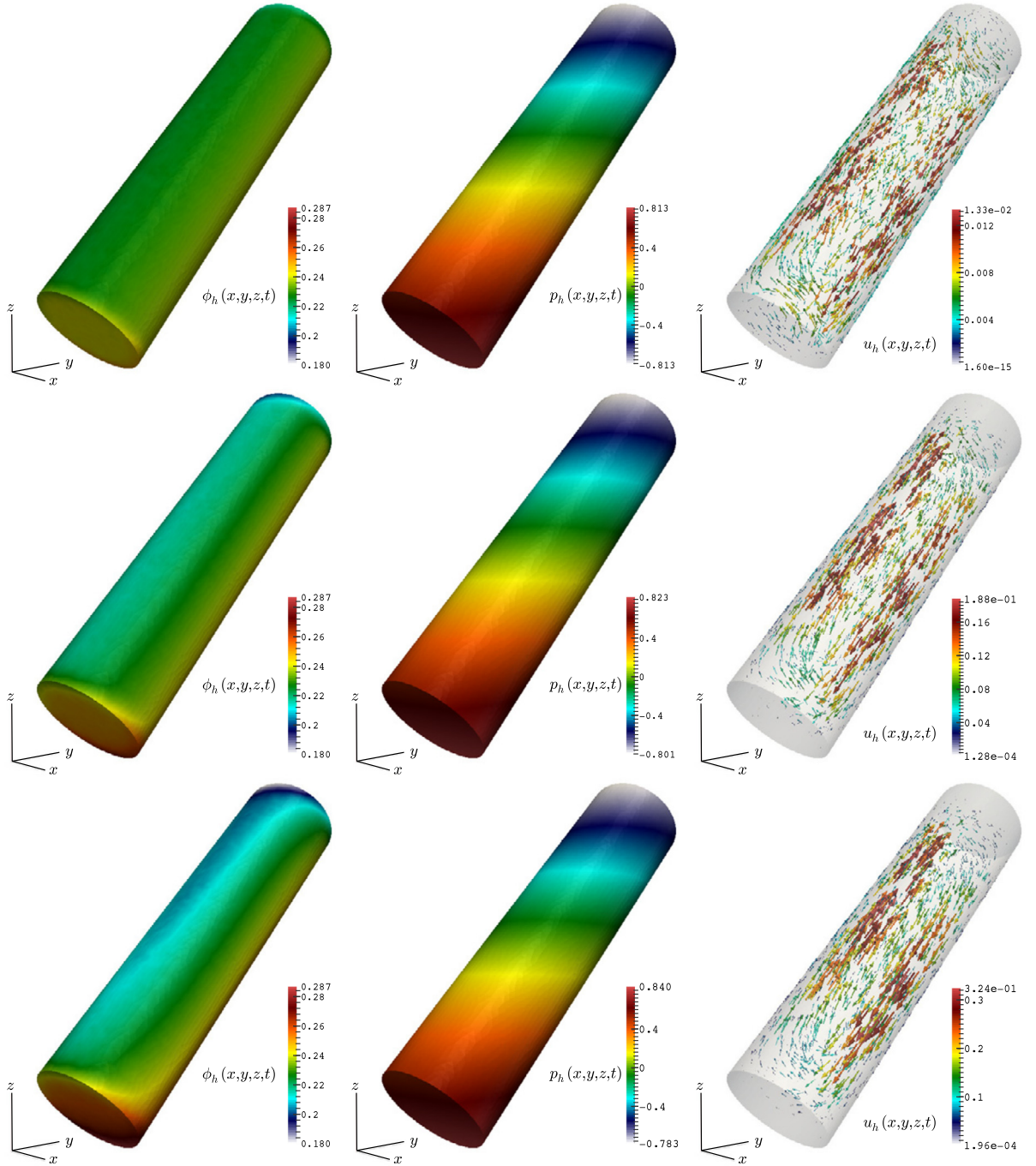


Fig. 10. Example 4: Discontinuous finite volume element approximations of concentration (left panels), pressure field (center), and velocity vectors (right) for the batch sedimentation process in a tilted cylinder. Snapshots at adimensional time instants $t = 5, 10, 16$ (top, middle, and bottom, respectively).

project CONICYT/FONDAP/15130015. SK is thankful to Cl²MA, Universidad de Concepción for providing financial support for a short term visit to that center, where the present work was substantially advanced. The work of RRB was supported by the Swiss National Science Foundation through the research grant PP00P2-144922.

Appendix A. Newton linearization

We apply a first-order backward Euler time stepping. For a fixed time $t = t^n < T$, we denote by $(\delta\phi_h^k, \delta\mathbf{u}_h^k, \delta p_h^k)$ an increment of the state $(\phi_h^k, \mathbf{u}_h^k, p_h^k)$ for $k = 1, \dots, k_{\max}$. This increment is the solution of the following linearization of (3.9)–(3.11):

$$\begin{aligned}
& \frac{1}{\Delta t} \langle \delta\phi_h^k, \mathcal{R}^\sharp \varphi_h \rangle + \mathcal{A}(\delta\phi_h^k, \varphi_h, \phi_h^k) + \int_{\Omega} \kappa'(\phi_h^k) \delta\phi_h^k \nabla \phi_h^k \cdot \nabla \varphi_h \, dx + \mathcal{C}(\phi_h^k, \varphi_h, \delta\mathbf{u}_h^k) + \mathcal{C}(\delta\phi_h^k, \varphi_h, \mathbf{u}_h^k) \\
&= -\frac{1}{\Delta t} \langle \phi_h^k, \mathcal{R}^\sharp \varphi_h \rangle - \mathcal{A}(\phi_h^k, \varphi_h, \phi_h^k) - \mathcal{C}(\phi_h^k, \varphi_h, \mathbf{u}_h^k) + \langle f, \varphi_h \rangle + \frac{1}{\Delta t} \langle \phi_h^{n-1}, \mathcal{R}^\sharp \varphi_h \rangle, \\
& \hat{\mathcal{A}}(\delta\mathbf{u}_h^k, \mathbf{v}_h; \phi_h^k) + \int_{\Omega} \mu'(\phi_h^k) \delta\phi_h^k \boldsymbol{\epsilon}(\mathbf{u}_h^k) : \boldsymbol{\epsilon}(\mathbf{v}_h) \, dx - b(\delta p_h^k, \mathbf{v}_h) - d(\delta\phi_h^k, \mathcal{P}^\sharp \mathbf{v}_h) \\
&= -\hat{\mathcal{A}}(\mathbf{u}_h^k, \mathbf{v}_h; \phi_h^k) + b(p_h^k, \mathbf{v}_h) + d(\phi_h^k, \mathcal{P}^\sharp \mathbf{v}_h) + \langle \mathbf{j}, \mathbf{v}_h \rangle, \\
& b(q_h, \delta\mathbf{u}_h^k) + b(q_h, \mathbf{u}_h^k) = 0,
\end{aligned} \tag{A.1}$$

for all $(\varphi_h, \mathbf{v}_h, q_h) \in \mathcal{S}_h \times \mathcal{V}_h \times \mathcal{Q}_h$, associated to homogeneous Dirichlet boundary conditions for the increment of velocity and concentration. The state at step k is assumed to satisfy the nonhomogeneous boundary datum imposed with the initial condition, and the overall loop is summarized in [Algorithm 1](#).

Algorithm 1 Solution algorithm.

```

1: Construct primal and dual meshes, set initial conditions  $\phi_h^0$ , Newton tolerance  $\epsilon$ , and global time step  $\Delta t$ 
2: for  $n = 1, \dots, N$  do
3:   set initial guess  $\phi_h^{k=0} \leftarrow \phi_h^{n-1}$ ,  $\mathbf{u}_h^{k=0} \leftarrow \mathbf{u}_h^{n-1}$ ,  $p_h^{k=0} \leftarrow 0$ 
4:   reset the norm of the increment  $\epsilon_R^{k=0} \leftarrow 2\epsilon$ 
5:   for  $k = 1, \dots, k_{\max}$  do
6:     given the values  $(\phi_h^k, \mathbf{u}_h^k, p_h^k)$ , find the increments  $(\delta\phi_h^k, \delta\mathbf{u}_h^k, \delta p_h^k)$  by solving (A.1)
7:     Compute the energy norm of the increment
      
$$\epsilon_R^k \leftarrow (\|\delta\phi_h^k\|_{1,\Omega}^2 + \|\delta\mathbf{u}_h^k\|_h^2 + \|\delta p_h^k\|_{0,\Omega}^2)^{1/2}$$

8:     Update the value of the approximation
      
$$\phi_h^n \leftarrow \delta\phi_h^k + \phi_h^k, \quad \mathbf{u}_h^n \leftarrow \delta\mathbf{u}_h^k + \mathbf{u}_h^k, \quad p_h^n \leftarrow \delta p_h^k + p_h^k$$

9:     if  $\epsilon_R^k < \epsilon$  or  $k \geq k_{\max}$  then
10:       break
11:     else
12:       continue
13:     end if
14:   end for
15: end for

```

Appendix B. Axisymmetric formulation for the sedimentation problem

Let $d = 3$. Under the assumption of cylindrical symmetry (with respect to the symmetry axis $\Gamma_s = \{r = 0\}$, cf. [Fig. 6](#)) of all the flow patterns, the expected concentration profiles, and the domain, the three-dimensional problem (1.1) in Cartesian coordinates (x, y, z, t) can be recast as the following two-dimensional system written in cylindrical coordinates (r, z, t) :

For all $t > 0$, find $\mathbf{u}(t) \in V_{1,\Gamma_s}^1(\Omega) \times H_{1,\Gamma}^1(\Omega)$, $p(t) \in L_{1,0}^2(\Omega)$ and $\phi(t) \in H_1^1(\Omega)$ such that

$$\begin{aligned}
& \partial_t \phi - \operatorname{div}_{\mathbf{a}}(\kappa(\phi) \nabla_{\mathbf{a}} \phi) + \mathbf{u} \cdot \nabla_{\mathbf{a}} \phi = \nabla_{\mathbf{a}} \cdot \mathbf{f}(\phi) \quad \text{in } \Omega \times (0, T), \\
& -\operatorname{div}_{\mathbf{a}}(\mu(\phi) \boldsymbol{\epsilon}_{\mathbf{a}}(\mathbf{u}) - p \mathbf{I}) - \phi \mathbf{g} = \mathbf{0} \quad \text{in } \Omega \times (0, T), \\
& \operatorname{div}_{\mathbf{a}} \mathbf{u} = 0 \quad \text{in } \Omega \times (0, T), \\
& \mathbf{u} = \mathbf{u}_{\Gamma} \quad \text{on } \Gamma \times (0, T), \\
& \phi = \phi_{\Gamma} \quad \text{on } \Gamma \times (0, T), \\
& \phi(0) = \phi_0 \quad \text{on } \Omega \times \{0\}.
\end{aligned}$$

Here the involved modified spaces are defined as follows (see details in e.g. [2,11,38]):

$$V_1^1(\Omega) := H_1^1(\Omega) \cap L_{-1}^2(\Omega), \quad V_{1,\Gamma_s}^1(\Omega) := \{w \in V_1^1(\Omega) : w = 0 \text{ on } \Gamma_s\},$$

$$L_{1,0}^2(\Omega) := \left\{ q \in L_1^2(\Omega) : \int_{\Omega} qr \, dr \, dz = 0 \right\},$$

where $L_{\alpha}^p(\Omega)$ denotes the space of measurable functions v on Ω such that

$$\|v\|_{L_\alpha^p(\Omega)}^p := \int_{\Omega} |v|^p r^\alpha \, dr \, dz < \infty,$$

$H_\alpha^m(\Omega)$ is the space of functions in $L_\alpha^p(\Omega)$ with derivatives up to order m also in $L_\alpha^p(\Omega)$, and $H_{\alpha,\Gamma}^m(\Omega)$ denotes its restriction to functions with null trace on a part of the boundary Γ . The modified differential operators are defined as

$$\nabla_a \mathbf{v} := \begin{bmatrix} \partial_r v_r & \partial_r v_z \\ \partial_z v_r & \partial_z v_z \end{bmatrix}, \quad \operatorname{div}_a \mathbf{v} := \partial_z v_z + \frac{1}{r} \partial_r(r v_r), \quad \boldsymbol{\epsilon}_a(\mathbf{v}) := \frac{1}{2} (\nabla_a \mathbf{v} + \nabla_a \mathbf{v}^T), \quad \nabla_a s = \begin{pmatrix} \partial_r s \\ \partial_z s \end{pmatrix}.$$

Moreover, all volume integrals in the definition of the DFVE formulation (3.9)–(3.11) have been replaced by their weighted counterparts, and the discrete spaces have been replaced by

$$\begin{aligned} \mathcal{V}_h^a &:= \left\{ \mathbf{v} \in V_1^1(\Omega) \times V_{1,\Gamma_s}^1(\Omega) : \mathbf{v}|_K \in \mathbb{P}_1(K)^d, \forall K \in \mathcal{T}_h \right\}, \\ \mathcal{Q}_h^a &:= \left\{ q \in L_{1,0}^2(\Omega) : q|_K \in \mathbb{P}_0(K), \forall K \in \mathcal{T}_h \right\}, \\ \mathcal{S}_h^a &:= \left\{ \varphi \in L_1^2(\Omega) : \varphi|_K \in \mathbb{P}_1(K), \forall K \in \mathcal{T}_h \right\}. \end{aligned}$$

References

- [1] S. Agmon, Lectures on Elliptic Boundary Value Problems, AMS, Providence, Rhode Island, 2010.
- [2] V. Anaya, D. Mora, C. Reales, R. Ruiz-Baier, Stabilized mixed approximation of axisymmetric Brinkman flows, *ESAIM: Math. Model. Numer. Anal.* 49 (2015) 855–874.
- [3] B. Andreotti, Y. Forterre, O. Pouliquen, Granular Media. Between Fluid and Solid, Cambridge University Press, Cambridge, UK, 2013.
- [4] D.N. Arnold, An interior penalty finite element method with discontinuous elements, *SIAM J. Numer. Anal.* 19 (1982) 724–760.
- [5] C. Bi, M. Liu, A discontinuous finite volume element method for second-order elliptic problems, *Numer. Methods Partial Differ. Equ.* 28 (2012) 425–440.
- [6] BIOMATH group, Ghent University, Private communication.
- [7] A.E. Boycott, Sedimentation of blood corpuscles, *Nature* 104 (1920) 532.
- [8] M. Brera, J.W. Jerome, Y. Mori, R. Sacco, A conservative and monotone mixed-hybridized finite element approximation of transport problems in heterogeneous domains, *Comput. Methods Appl. Mech. Eng.* 199 (2010) 2709–2720.
- [9] R. Bürger, S. Diehl, Convexity-preserving flux identification for scalar conservation laws modelling sedimentation, *Inverse Probl.* 29 (2013) 045008 (30 pp.).
- [10] R. Bürger, S. Diehl, I. Nopens, E. Torfs, A consistent modelling methodology for secondary settling tanks: a reliable numerical method, *Water Sci. Technol.* 68 (2013) 192–208.
- [11] R. Bürger, R. Ruiz-Baier, H. Torres, A stabilized finite volume element formulation for sedimentation-consolidation processes, *SIAM J. Sci. Comput.* 34 (2012) B265–B289.
- [12] R. Bürger, W.L. Wendland, F. Concha, Model equations for gravitational sedimentation-consolidation processes, *Z. Angew. Math. Mech.* 80 (2000) 79–92.
- [13] Z. Cai, On the finite volume element method, *Numer. Math.* 58 (1991) 713–735.
- [14] P. Chatzipantelidis, V. Ginting, A finite volume element method for a nonlinear parabolic problem, in: O.P. Iliev, S.D. Margenov, P.D. Minev, P.S. Vassilevski, L.T. Zikatanov (Eds.), Numerical Solution of Partial Differential Equations: Theory, Algorithms, and Their Applications, Springer, New York, 2013, pp. 121–136.
- [15] P. Chatzipantelidis, V. Ginting, R.D. Lazarov, A finite volume element method for a nonlinear elliptic problem, *Numer. Linear Algebra Appl.* 12 (2005) 515–546.
- [16] S.C. Chou, Analysis and convergence of a covolume method for the generalized Stokes problem, *Math. Comput.* 66 (1997) 85–104.
- [17] M. Cui, X. Ye, Unified analysis of finite volume methods for the Stokes equations, *SIAM J. Numer. Anal.* 48 (2010) 824–839.
- [18] G.A. Ekama, J.L. Barnard, F.W. Günther, P. Krebs, J.A. McCorquodale, D.S. Parker, E.J. Wahlberg, Secondary Settling Tanks: Theory, Modelling, Design and Operation, Scientific and Technical Report 6, International Association on Water Quality, London, 1997.
- [19] R.E. Ewing, T.F. Russell, Efficient time-stepping methods for miscible displacement problems in porous media, *SIAM J. Numer. Anal.* 19 (1982) 1–67.
- [20] F. Gao, Y. Yuan, D. Yang, An upwind finite-volume element scheme and its maximum-principle-preserving property for nonlinear convection-diffusion problem, *Int. J. Numer. Methods Fluids* 56 (2008) 2301–2320.
- [21] E.S. Gross, L. Bonaventura, G. Rosatti, Consistency with continuity in conservative advection schemes for free-surface models, *Int. J. Numer. Methods Fluids* 38 (2002) 307–327.
- [22] A. Guardone, L. Vigevano, Finite element/volume solution to axisymmetric conservation laws, *J. Comput. Phys.* 224 (2007) 489–518.
- [23] E. Guazzelli, J. Hinch, Fluctuations and instability in sedimentation, *Annu. Rev. Fluid Mech.* 43 (2011) 97–116.
- [24] E. Guazzelli, J.E. Morris, A Physical Introduction to Suspension Dynamics, Cambridge University Press, 2012.
- [25] T. Gudi, N. Nataraj, A.K. Pani, hp-Discontinuous Galerkin methods for strongly nonlinear elliptic boundary value problems, *Numer. Math.* 109 (2008) 233–268.
- [26] R. Jackson, The Dynamics of Fluidized Particles, Cambridge University Press, 2000.
- [27] S. Kumar, A mixed and discontinuous Galerkin finite volume element method for incompressible miscible displacement problems in porous media, *Numer. Methods Partial Differ. Equ.* 28 (2012) 1354–1381.
- [28] S. Kumar, On the approximation of incompressible miscible displacement problems in porous media by mixed and standard finite volume element methods, *Int. J. Model. Simul. Sci. Comput.* 4 (2013) 1350013 (30 pp.).
- [29] S. Kumar, N. Nataraj, A.K. Pani, Discontinuous Galerkin finite volume element methods for second order linear elliptic problems, *Numer. Methods Partial Differ. Equ.* 25 (2009) 1402–1424.
- [30] S. Kumar, R. Ruiz-Baier, Equal order discontinuous finite volume element methods for the Stokes problem, *J. Sci. Comput.* (2015), <http://dx.doi.org/10.1007/s10915-015-9993-7>, in press.
- [31] D. Kuzmin, Y. Gorb, A flux-corrected transport algorithm for handling the close-packing limit in dense suspensions, *J. Comput. Appl. Math.* 236 (2012) 4944–4951.
- [32] G.J. Kynch, A theory of sedimentation, *Trans. Faraday Soc.* 48 (1952) 166–176.
- [33] R.H. Li, Generalized difference methods for a nonlinear Dirichlet problem, *SIAM J. Numer. Anal.* 24 (1987) 77–88.
- [34] J. Li, Z. Chen, A new stabilized finite volume method for the stationary Stokes equations, *Adv. Comput. Math.* 30 (2009) 141–152.
- [35] S.J. Lin, R.B. Rood, Multidimensional flux-form semi-Lagrangian transport schemes, *Mon. Weather Rev.* 124 (1996) 2046–2070.

- [36] S.A. Lorca, J.L. Boldrini, The initial value problem for a generalized Boussinesq model, *Nonlinear Anal.* 36 (1999) 457–480.
- [37] Z.D. Luo, A stabilized Crank–Nicolson mixed finite volume element formulation for the non-stationary incompressible Boussinesq equations, *J. Sci. Comput.* (2015), <http://dx.doi.org/10.1007/s10915-015-0034-3>, in press.
- [38] B. Mercier, G. Raugel, Resolution d'un problème aux limites dans un ouvert axisymétrique par éléments finis en r , z et séries de Fourier en t , *RAIRO. Anal. Numér.* 16 (1982) 405–461.
- [39] M.R. Ohm, H.Y. Lee, J.Y. Shin, Error estimates for discontinuous Galerkin methods for nonlinear parabolic problems, *J. Math. Anal. Appl.* 315 (2006) 132–143.
- [40] A. Quarteroni, R. Ruiz-Baier, Analysis of a finite volume element method for the Stokes problem, *Numer. Math.* 118 (2011) 737–764.
- [41] J.F. Richardson, W.N. Zaki, Sedimentation and fluidization: Part I, *Trans. Inst. Chem. Eng. (Lond.)* 32 (1954) 35–52.
- [42] B. Rivière, M.F. Wheeler, V. Girault, A priori error estimates for finite element methods based on discontinuous approximation spaces for elliptic problems, *SIAM J. Numer. Anal.* 39 (2001) 902–931.
- [43] R. Ruiz-Baier, I. Lunati, Mixed finite element–primal finite volume element discretization of multicontinuum models, 2015, submitted for publication.
- [44] R. Ruiz-Baier, H. Torres, Numerical solution of a coupled flow–transport system modeling multidimensional sedimentation processes, *Appl. Numer. Math.* 95 (2015) 280–291.
- [45] S. Saha, D. Salin, L. Talon, Low Reynolds number suspension gravity currents, *Eur. J. Phys. E* 36 (2013) 85 (18 pp.).
- [46] C. Schär, P.K. Smolarkiewicz, A synchronous and iterative flux-correction formalism for coupled transport equations, *J. Comput. Phys.* 128 (1996) 101–120.
- [47] S. Sun, B. Rivière, M.F. Wheeler, A combined mixed finite element and discontinuous Galerkin method for miscible displacement problem in porous media, in: T.F. Chan, Y. Huang, T. Tang, J. Xu, L.-A. Ying (Eds.), *Recent Progresses in Computational and Applied PDEs*, Proceedings of the International Conference, Zhangjiajie, July 2001, Kluwer Academic/Plenum Publishers, New York, 2002, pp. 321–348.
- [48] M. Ungarish, *An Introduction to Gravity Currents and Intrusions*, CRC Press, Boca Raton, FL, 2009.
- [49] J. Wen, Y. He, J. Yang, Multiscale enrichment of a finite volume element method for the stationary Navier–Stokes problem, *Int. J. Comput. Math.* 90 (2013) 1938–1957.
- [50] B.A. Wills, T. Napier-Munn, *Wills Mineral Processing Technology*, seventh ed., Butterworth-Heinemann/Elsevier, Oxford, UK, 2006.
- [51] J. Xu, L. Zikatanov, A monotone finite element scheme for convection–diffusion equations, *Math. Comput.* 68 (1999) 1429–1446.
- [52] Q. Yang, Z. Jiang, A discontinuous mixed covolume method for elliptic problems, *J. Comput. Appl. Math.* 235 (2011) 2467–2476.
- [53] X. Ye, A new discontinuous finite volume method for elliptic problems, *SIAM J. Numer. Anal.* 42 (2004) 1062–1072.
- [54] X. Ye, A discontinuous finite volume method for the Stokes problem, *SIAM J. Numer. Anal.* 44 (2006) 183–198.